

University of Nevada, Reno

**A New Three-Dimensional Rockfall Trajectory Simulator for Open-
Pit Mines**

A thesis submitted in partial fulfilment of the requirements for the degree
of Master of Science in Mining Engineering

By:

Bijan Peik

Dr. Behrooz Abbasi/Thesis Advisor

Dr. Javad Sattarvand/Thesis Co-Advisor

May 2020

Copyright © by Bijan Peik 2020

All Rights Reserved



THE GRADUATE SCHOOL

We recommend that the thesis
prepared under our supervision by

BIJAN PEIK

entitled

**A New Three-Dimensional Rockfall Trajectory Simulator
for Open-Pit Mines**

be accepted in partial fulfillment of the
requirements for the degree of

MASTER OF SCIENCE

Behrooz Abbasi, Ph.D., *Advisor*

Javad Sattarvand, Ph.D., *Co-advisor*

Robert Watters Ph.D., *Committee Member*

Sean Warren, Ph.D., *Committee Member*

Rajaratnam Siddharthan, Ph.D., *Graduate School Representative*

David W. Zeh, Ph.D., Dean, *Graduate School*

May, 2020

AN ABSTRACT OF THE THESIS OF

Bijan Peik, for the Master of Science Degree in Mining Engineering, at University of Nevada, Reno

Title: A New Three-Dimensional Rockfall Trajectory Simulator for Open-Pit Mines

Major advisors: Dr. Behrooz Abbasi (Advisor) and Dr. Javad Sattarvand (Co-advisor)

Background. Rockfall hazards on open-pit highwalls are composed of two major associated risks, the chance of the rockfall itself and the area impacted by falling rock blocks or the runout zone. Rockfall trajectory assessment is essential for estimating consequences of such incidents. Several simulation techniques in the form of computer programs have been developed for this purpose. They are used to obtain the required basis for protection designs and safety considerations in rockfall prone areas.

Innovations. In this thesis, a new three-dimensional analytical program was developed for rockfall trajectory simulation and estimating runout zones. This program is designed to effectively read and visualize topographies composed of large numbers of mesh elements. It utilizes special algorithms to enable fast and effective simulations of high-resolution terrain models. The output generated by this program includes rockfall trajectories providing bounce heights, rockfall velocities and impact locations for safety designs and rock trace maps that identify hazardous zones. Both may be used by operations management to designate safe working stations in open-pit mines.

Results. The developed program was calibrated using small-scale bounce tests where a detailed study was conducted on the efficiency of the program to accurately simulate

bounce heights and lengths. Moreover, the performance of the program was examined in an actual open-pit mine to highlight specific capabilities of incorporated algorithms for trajectory modeling and processing high-resolution terrain models. Based on results from the case study, the program's modeling showed acceptable correspondence to experimental results as well as reliable performance in trajectory simulation of rockfalls in terms of time-effective analysis and reasonable outcome given assumptions and input parameters.

DEDICATION

It is not about dedication, as those who I am pointing at own not only this, but also everything that I have ever accomplished and all my love. Those are the ones that I looked up to as a teenager, and now look forward to as a young adult. My family, kindest people I have ever seen, are the ones I want to make the most proud of me. I won't stop making you happy!

ACKNOWLEDGEMENTS

I would like to express my sincere gratitude and indebtedness to my adviser Dr. Behrooz Abbasi, and my co-advisor Dr. Javad Sattarvand for their inspiring guidance and valuable suggestions throughout these project works. I would not have had the opportunity to grow and conquer without their unfailing support.

The research conducted in this thesis is part of a five-year project titled “Capacity Building in Artificially Intelligent Mining Systems (AIMS) for Safer and Healthier Automated Operations” funded by National Institute for Occupational Health and Safety (NIOSH).

I am thankful to Prof. Raj Siddharthan, Prof. Robert Watters, and Dr. Sean Warren for serving on my committee and providing me with valuable comments. Moreover, special thanks to Dr. Masoud Zare Naghadehi, Mr. Rushikesh Battulwar, and Mr. Mohammadreza Soltany Sadrabadi for their support and contribution to publishing the results of this study.

I would also like to gratefully thank my kindest friend Dr. Saeed Ahmadvand for all of his support, motivation and kind words in difficult times.

In the end, special thanks go to all faculty members of Department of Mining Engineering at the University of Nevada, Reno for their support.

TABLE OF CONTENT

AN ABSTRACT OF THE THESIS OF.....	I
DEDICATION.....	III
ACKNOWLEDGEMENTS.....	IV
TABLE OF CONTENT.....	V
TABLE OF FIGURES.....	IX
TABLE OF TABLES.....	VIII
CHAPTER 1 : INTRODUCTION.....	1
1.1 BACKGROUND AND NEED FOR THIS STUDY	1
1.2 STATEMENT OF PROBLEM	2
1.3 GOALS AND SPECIFIC OBJECTIVES	3
1.4 OVERALL APPROACH	4
1.5 THESIS ORGANIZATION	6
CHAPTER 2 : LITERATURE REVIEW.....	7
2.1 ROCKFALL TRAJECTORY ASSESSMENT	7
2.2 ROCKFALL MECHANISM.....	8
2.2.1 <i>Parabolic Equations</i>	10
2.2.2 <i>Rock-ground Interaction Mechanics</i>	10
2.2.3 <i>Restitution Coefficients</i>	12
2.3 ROCKFALL EXPERIMENTAL ANALYSIS	13
2.4 PROBABILISTIC MODELLING	15
2.5 COMPUTER SIMULATION	16
2.5.1 <i>STONE and Hy-STONE</i>	18
2.5.2 <i>Rockfall Analyst</i>	21
2.5.3 <i>CRSP3D</i>	25

2.5.4	<i>Rockyfor3D</i>	26
2.5.5	<i>RAMMS:: ROCKFALL MODULE</i>	29
2.6	SUMMARY	32
CHAPTER 3 : PROGRAM DEVELOPMENT.....		34
3.1	RPF3D INPUT PARAMETERS	34
3.2	RPF3D TERRAIN MODEL	36
3.3	RPF3D TRAJECTORY MODELING	38
3.4	RPF3D IMPACT DETECTION.....	42
3.5	RPF3D STOPPING CRITERION	43
3.6	SUMMARY	43
CHAPTER 4 : EXPERIMENTAL ANALYSIS AND RPF3D CALIBRATION/VALIDATION		
44		
4.1	EXPERIMENTAL SETUP	44
4.2	OBJECT TRACKING	46
4.3	EXPERIMENTAL TRIALS.....	48
4.4	RPF3D SIMULATIONS AND EXPERIMENTAL COMPARISON.....	48
4.5	COMPARATIVE ANALYSIS RESULTS AND MODEL VALIDATION.....	50
4.6	SUMMARY	53
CHAPTER 5 : APPLICATION OF RPF3D AT AN OPEN-PIT MINE.....		54
5.1	ARTURO OPEN-PIT MINE	54
5.2	RFP3D ROCKFALL SIMULATION RESULTS.....	56
5.2.1	<i>Effect of local bench spills on the trajectory of the rockfall</i>	62
5.3	SUMMARY	66
CHAPTER 6 : CONCLUSIONS AND RECOMMENDATIONS		68
6.1	RESEARCH SUMMARY	68

6.2 RESEARCH RESULTS.....68

6.3 RECOMMENDATIONS FOR ADDITIONAL RESEARCH69

REFERENCES.....71

APPENDIX77

TABLE OF TABLES

TABLE 2-1 DIFFERENT KINETIC MODELS' MOTION AND FORCE CONSIDERATIONS.	9
TABLE 2-2 AN OVERVIEW OF THE CURRENT ROCKFALL SIMULATION PROGRAMS AND RPF3D.	33
TABLE 3-1 GENERAL ASSUMPTIONS OF RPF3D.	34
TABLE 4-1 INPUT PARAMETERS FOR LAB TEST SIMULATION.	49
TABLE 5-1 MODEL INPUTS AND SPECIFIC PARAMETERS FOR THE TRAJECTORY COMPUTATION	57
TABLE 5-2 COMPARATIVE STUDY BETWEEN TWO RESOLUTIONS OF THE TERRAIN MODEL	59
TABLE 5-3 THE COR VALUES FOR EACH GEOLOGY UNIT.	63
TABLE 5-4 RESULTS OF THE COMPARATIVE STUDY FOR COR GENERALIZING AND LOCALIZING.	66

TABLE OF FIGURES

FIGURE 1-1 FLOWCHART OF RESEARCH APPROACH.....	5
FIGURE 2-1 DIFFERENT KINEMATIC CONCEPTS IN ROCKFALL MODELING.	9
FIGURE 2-2 ILLUSTRATION OF VELOCITY VECTORS TRANSFORMATION ACCORDING TO PLANE DIP AND TREND (MODIFIED FROM LAN ET AL., 2007).	11
FIGURE 2-3 ILLUSTRATION OF HOW RESTITUTION COEFFICIENTS AFFECT ROCK TRANSLATIONAL VELOCITY (MODIFIED FROM WYLLIE, 2014).....	13
FIGURE 2-4 STONE RASTER OUTPUTS SHOWING (A) NUMBER OF ROCKFALL TRAJECTORIES, (B) MAXIMUM ROCKFALL VELOCITIES RANGING FROM 50 KM.H ⁻¹ (GREEN) TO MORE THAN 300 KM.H ⁻¹ (RED), (C) MAXIMUM HEIGHT TRAJECTORIES ABOVE GROUND RANGING FROM 5M TO 100M.	19
FIGURE 2-5 DEFINITION OF THE PLANE COORDINATE SYSTEM ASSOCIATED WITH NEIGHBORING CELLS.....	22
FIGURE 2-6 TRAJECTORIES FOR FOUR SOURCE AREAS WITH SOURCES 1 AND 2 EXHIBITING THE HIGHEST HAZARD TO RAILWAY TRACKS.	24
FIGURE 2-7 ROCKFALL TRAJECTORIES CONSIDERING A CONCRETE BARRIER IN THEIR PATH TO THE RAILWAY TRACK.	24
FIGURE 2-8 CRSP3D OUTPUT: ROCKFALL SOURCE LOCATIONS AND TRAJECTORIES (NUGRAHA ET AL., 2017).	26
FIGURE 2-9 POSSIBLE LATERAL DISPERSION OF THE ROCK WHEN IMPACTING THE SLOPE.....	28
FIGURE 2-10 ILLUSTRATION OF THE SCARRING PHENOMENA (MODIFIED FROM DORF, 2019).	30
FIGURE 2-11 RAMMS 3D OUTCOME OVERVIEW (SCHWEIZER ET AL., 2013).....	32
FIGURE 3-1 STL FORMAT GEOMETRY.	36
FIGURE 3-2 VTK POLY DATA WITH ID NUMBER FOR EACH TRIANGLE.	38
FIGURE 3-3 A) SAMPLE TRAJECTORIES AND TRACE-MAP GENERATED BY RPF3D, B) 2D CROSS-SECTION GENERATED FOR ONE OF THE TRAJECTORIES ALONG WITH C) ROCK VELOCITY THROUGHOUT THE TRAJECTORY.....	40

FIGURE 3-4 CODE STRUCTURE SHOWING DATA INPUT, TERRAIN MODEL, ROCK MOTION, IMPACT DETECTION, AND STOPPING CRITERION ALGORITHMS.	41
FIGURE 4-1 ADJUSTABLE SLOPE SETUP FOR ROCKFALL TESTING.....	45
FIGURE 4-2 MODEL SETUP, REALISING LOCATION OF THE PING-PONG BALL, AND AN INDICATION OF THE OBJECT-TRACKING DETECTION OF THE BALL.	47
FIGURE 4-3 OBJECT TRACKING SAMPLE USING OPENCV. THE BALL COLOR IS USED TO TRACK THE OBJECT AND THE TRAJECTORY IS SUPERPOSED.	48
FIGURE 4-4 THE SIMULATIONS OUTCOME FOR A)22, B)40, C)50, AND D)59° SLOPE ANGLES.	49
FIGURE 4-5 OBJECT TRACKING AND COMPUTER MODELING RESULTS FOR 22° SLOPE ANGLE	51
FIGURE 4-6 OBJECT TRACKING AND COMPUTER MODELING RESULTS FOR 40° SLOPE ANGLE.	51
FIGURE 4-7 OBJECT TRACKING AND COMPUTER MODELING RESULTS FOR 50° SLOPE ANGLE.	52
FIGURE 4-8 OBJECT TRACKING AND COMPUTER MODELING RESULTS FOR 59° SLOPE ANGLE.	52
FIGURE 5-1 A)LOCATION MAP OF THE ARTURO MINE, B)OPEN-PIT MINE DESIGN MAP FOR THREE PHASES OF SOUTH ARTURO MINE (MIRANDA ET AL., 2018).	55
FIGURE 5-2 MOSAIC AERIAL PHOTO OF THE ARTURO WEST BUTTON HILL (PHASE 2)(BATTULWAR ET AL., 2019).....	56
FIGURE 5-3 A) 3D TERRAIN MODEL, B) TRIANGLES FROM THE HIGH-RESOLUTION MODEL (~1 M EDGE SIZE), AND C) TRIANGLES FROM THE LOW RESOLUTION MODEL (~7 M EDGE SIZE).....	57
FIGURE 5-4 ROCKFALL TRAJECTORIES FOR HIGH-RESOLUTION TERRAIN.....	58
FIGURE 5-5 ROCKFALL TRAJECTORIES FOR LOW-RESOLUTION TERRAIN.	59
FIGURE 5-6 LOW-RESOLUTION PIT GEOMETRY, ROCKFALL TRAJECTORIES, AND RUNOUT ZONES.	60
FIGURE 5-7 HIGH-RESOLUTION PIT GEOMETRY, ROCKFALL TRAJECTORIES, AND RUNOUT ZONES.	61
FIGURE 5-8 COMPARISON BETWEEN THE OUTCOME FOR THE LOW AND HIGH RESOLUTION OF THE INPUT TERRAIN MODEL.	62
FIGURE 5-9 A GRAPHICAL VIEW OF THE BENCH SCALE FAILURES (SPILLS) ON THE SLOPE WALLS (RED AREAS).	62
FIGURE 5-10 DIFFERENT GEOLOGICAL SETTINGS AND SPILLS DETECTED IN RED COLOR.	63

FIGURE 5-11 ROCKFALL TRAJECTORIES ON THE NEW TERRAIN MODEL WITH LOCALIZED CORs.....64

FIGURE 5-12 CLOSE VIEW OF THE ROCKFALL TRACE MAP A) IN A LOCALIZED COR CONSIDERATION VS B)
GENERALIZED COR.65

FIGURE 5-13 COMPARISON BETWEEN THE TWO METHODS OF DEFINING COEFFICIENTS OF RESTITUTION.....66

CHAPTER 1 : INTRODUCTION

1.1 Background and Need for This Study

Many terms have been used by researchers to describe rockfalls, such as complex natural phenomenon, catastrophic geo-hazard, and common-place geomorphological process. Rockfalls occur when a rock block is detached from natural or engineered slopes (Basson, 2012). Mountainous road cuts, quarry faces, and open-pit mines are highly subject to rockfalls (Agliardi & Crosta, 2003; Chen et al., 2013). Rockfalls along slope walls have led to loss of human lives and infrastructure in past years. Their occurrence is inevitable even on stable slope benches in open-pit mines.

Normal mining operations can escalate the risk of rockfalls from highwalls leading to the need for a systematic approach to identifying rockfall risk and evaluating its potential consequences. Developing hazard maps and installing protective measures such as nets and dams (Peila et al., 1998) are important efforts used in addressing and mitigating rockfall incidents. For these tools and techniques to be effective, different aspects of rockfalls need to be rigorously studied and understood, including rockfall risk assessments, run-out distances, bounce heights and lengths, and lateral dispersion of falling rocks (Cruden & Varnes, 1996; Whalley, 1984). Hence, experimental and computational simulations have been increasingly utilized to assist with rockfall assessment and mitigation.

The literature review in Chapter 2 provides an overview of several programs that have been developed for rockfall trajectory simulation. They can be categorized based on terrain and simulation properties. Terrain input can be either a two-dimensional (2D) profile (Stevens, 1998) or three-dimensional (3D) geometry (Bourrier et al., 2009; Christen et al.,

2012; Crosta and Agliardi, 2004; Guzzetti et al., 2003; Guzzetti et al., 2002; Lan et al., 2007; Pfeiffer and Higgins, 1990). Simulation properties include three different methods for analyzing rockfall kinetics. They are lumped mass, hybrid (rigid sphere), and complex rigid body.

Looking at a single rockfall phenomenon in detail, its trajectory is composed of four stages: free fall, bouncing, rolling, and sliding. The first stage follows Newton's law based on gravity; however, uncertainties emerge when the rock collides with the slope surface (L. K. A. Dorren, 2003). The rock-ground interaction and the energy dissipation that occurs are very challenging to accurately simulate as both rock and slope mechanical, geometrical, and physical properties are hard to obtain due to hazards associated with falling rocks and the huge areal extent that rockfall paths can cover (Lan et al., 2007).

1.2 Statement of Problem

In a 2D simulation, the rock-slope interaction cannot be modeled realistically as the rock shape and slope dip direction are not considered. This has been addressed by 3D simulations in recently developed programs. Counterintuitively, complex dynamic analysis may not provide the desired outcome as there are uncertainties in model parameters such as the exact shape, mass, and size of the rock boulder and terrain model properties. Moreover, extensive computation time is required for such analysis (Pfeiffer and Higgins, 1990). The rigid body (sphere) method also exhibits overestimated results as the spherical rock keeps rolling on an inclined slope (Schweizer et al., 2013). Meanwhile, a reliable and fast method is required in open-pit mines where the complex dynamic analysis of rockfalls is not applicable due to the lack of detailed input parameters. Furthermore, as high risk is

associated with rockfall incidents in open-pit mines, primitive methods are incapable of providing the required basis for rockfall safety measures. Hence, the reliability of current computer programs to be used as a primary reference for rockfall analysis in open-pit mines is still unsettled.

1.3 Goals and Specific Objectives

This research is part of an automated rockfall risk alert system (ARRAS), which attempts to simulate rockfall paths, find run-out zones, and mark them as a hazard map for use in mining operations. The main objective of this study is to develop a methodology to generate a “Hazard Map” for a given open-pit mine based on identified rockfall runout zones. A new 3D computer program, Rock PathFinder (RPF3D), was developed implementing lumped mass method and semi-empirical elasticity for rock-surface impact. RPF3D is designed in accordance with specific conditions in an open-pit mine to provide a handy and reliable tool for rockfall hazard risk assessment.

In this thesis, a comprehensive overview of the developed program is given along with assumptions, limitations, and a step-by-step analysis of the RPF3D algorithm. Simplified small-scale bounce tests were designed to evaluate the accuracy of the program in measuring bounce heights and lengths. A case study was also analyzed to show the performance of this program in rockfall trajectory simulation for open-pit mines. Additionally, a study on the influence of different terrain model resolutions, along with a discussion on the use of generalized coefficients of restitution (COR) versus localized CORs are presented to highlight the capabilities of the program and provide useful context for future trajectory simulations.

Goals of this study are as follow:

- Fill the gap between open-pit mining needs and available rockfall assessment tools.
- Develop a rockfall trajectory simulation tool using advanced programming techniques.
- Calibrate the developed program with detailed small-scale bounce experiments.
- Solve the time-consuming task of reading high-resolution terrain models.
- Evaluate the effect of spills on rockfall trajectories.

1.4 Overall Approach

To achieve the previously mentioned objectives, three tasks were designed and the overall approach is summarized in Figure 1-1.

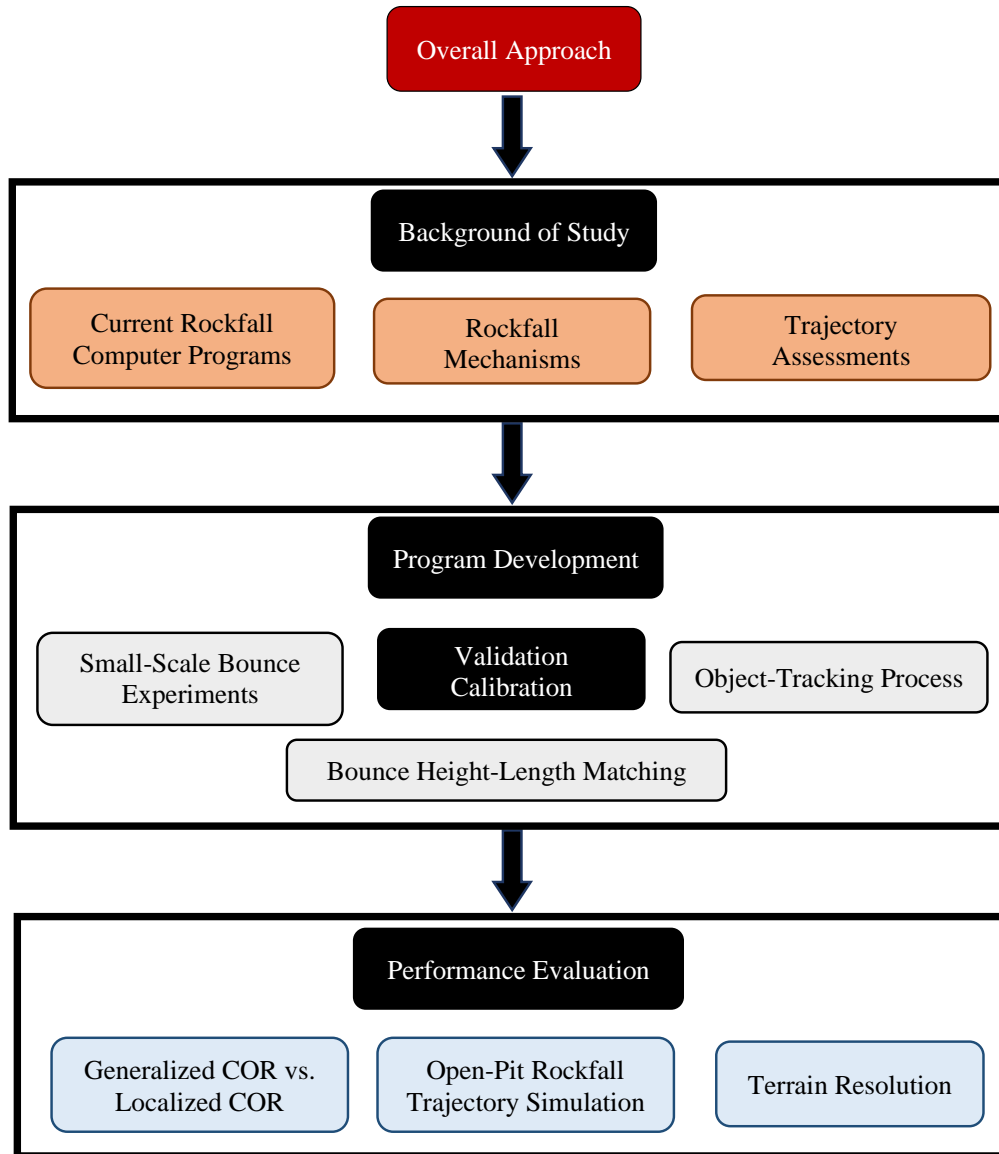


Figure 1-1 Flowchart of research approach.

- Task1: Develop a rockfall simulation computer program in Python that overcomes limitations involved with high-resolution terrain models and optimizes conventional outcomes of rockfall simulators to meet the needs of open-pit mines.
- Task 2: Design small-scale laboratory rockfall tests to calibrate the program in a detailed process. Analyze bounce heights and lengths of an object in the lab and

find errors between tracking results and simulation outcomes associated with surface COR assumptions and the kinetic approach used in RPF3D.

- Task 3: Evaluate the performance of the program in simulating rockfall trajectories for an open-pit mine. Compare outcomes of trajectory simulation for high- and low-terrain resolutions to emphasize the importance of surface geometry. This task will provide a discussion on the two types of considerations for CORs in trajectory simulation by analyzing the spills effect on rockfall runout zones.

1.5 Thesis Organization

This thesis contains six chapters. Chapter organization is as follows:

- Chapter 1– Introduction and problem statement.
- Chapter 2 – Review of rockfall modeling and major trajectory simulation programs.
- Chapter 3 – Overview of assumptions, capabilities, limitations, and a detailed analysis of algorithms used in the developed program.
- Chapter 4 – Experimental design used for validation and calibration of the developed program.
- Chapter 5 – Case study to evaluate the performance of the developed program and highlight its key advantages.
- Chapter 6 – Conclusions and recommendations.
- Appendix – The RPF3D source code implementation.

CHAPTER 2 : LITERATURE REVIEW

Due to severe consequences of rockfall events, this phenomenon has been extensively analyzed by several researchers. Rockfall analysis has two aspects: rockfall risk estimation and trajectory assessment. The main focus of this research is rockfall path analysis and runout modelling. This chapter presents a comprehensive review of the major research concerning these subjects. It is divided into following subsections based on relevance to the research topic. 1) rockfall trajectory assessments, 2) rockfall mechanisms, 3) kinetic relations, 4) rock-ground interaction mechanics, and 5) rockfall computer programs.

2.1 Rockfall Trajectory Assessment

Stability analysis in open-pit mines involves different techniques and methods to provide a balance between safe and economic mining. Rockfalls are among the critical and prevalent challenges in such studies. Although open-pit highwalls are designed to prevent large-scale slope failures, rockfall incidents can still cause safety concerns for mining operations. Safety considerations related to this issue require proper estimation of the risk of rockfalls on pit walls and a realistic assessment of rockfall trajectories and their potential runout zones; however, due to high uncertainty associated with the rockfall phenomenon, a reliable method that can be used as the primary reference for rockfall analysis is still unsettled.

The first systematic study of rockfall trajectories was based on full-scale experiments (Ritchie, 1963). Back analysis of rockfall instances was another approach in early attempts to address this phenomenon. *In situ* observations and back analysis of rockfalls led to the development of empirical and statistical models for rockfall hazard assessments

(Heidenreich, 2004). Empirical studies were mainly based on large-scale tests as Ritchie studied different slope angles over which rock boulders roll, bounce, or fall vertically. In another large-scale experiment, empirical correlations between rock volume and rebound height and lateral dispersion were found (Broili, 1976). In addition, Lied (1977) developed a criterion for the maximum distance travelled by rocks in a rockfall incident by back analyzing several rockfall events. Other researchers also used back analysis to gain information about rockfall trajectories that provided valuable data for runout distances, as well as bounce height and length ranges for various block sizes (Cui et al., 2017; Giani et al., 2004; Matasci et al., 2018).

One of the most important stages in rockfall trajectory assessment is the physical analysis of different kinematical and mechanical phenomena that exist throughout a rockfall incident. The analytical investigation of rock motion and rock-ground kinetics help in the characterization of the contributing parameters and leads to reliable simulations of the real physical phenomenon. Hence, an overview of the physical and kinematical relations involved in rockfall is given in section 2.2.

2.2 Rockfall Mechanism

As mentioned in the introduction, the rockfall phenomenon can be divided into four stages: free fall, bounce (impact), rolling, and sliding. The impact stage can also have two stages, scaring and slipping (Dorf, 2019). Rock motion including free fall and flying after each bounce is controlled by Newton's law and gravity. Forces acting on the rock and surface contact are modeled in different approaches according to the availability of physical parameters in the field and the level of complexity of the model. There are three

different methods for analyzing rockfall kinetics as shown in Figure 2-1. These include lumped mass method, hybrid method (rigid sphere), and complex rigid body. The lumped mass approach considers the rock as a point of mass and only accounts for its translational behavior, while the hybrid method considers a spherical shape for the rock in the rebound computation for which the angular velocity vector is defined. Finally, in the complex rigid body approach, the rock is defined by a set of geometrical parameters, a center of mass, and an inertia tensor.

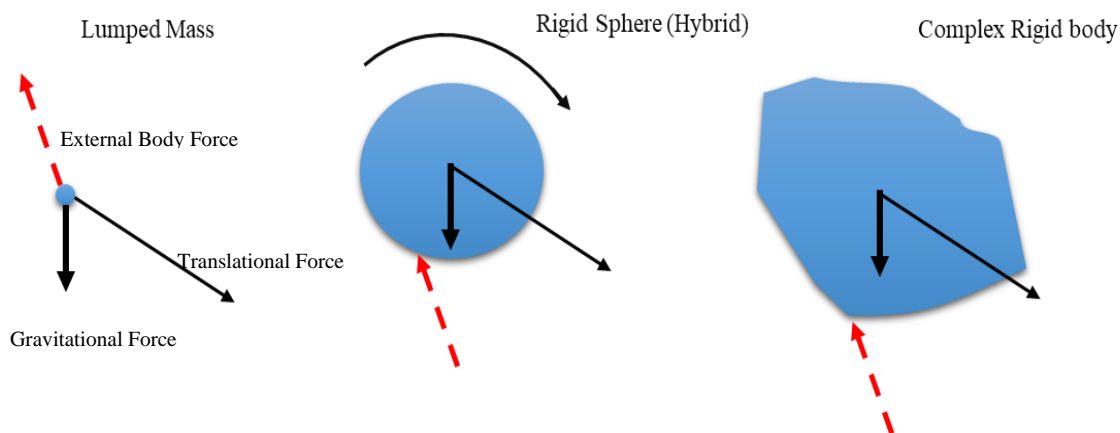


Figure 2-1 Different kinematic concepts in rockfall modeling.

Vertical downward arrows in Figure 2-1 are the direction of gravity, and red dashed arrows show external body forces. The oblique black arrows also indicate rock motion direction. Specifications for each kinetic method are summarized in Table 2-1.

Table 2-1 Different kinetic models' motion and force considerations.

Rock	Mass point	Rigid Sphere	Irregular rigid polygon
Motion	Translation	Translation and Rotation	Translation and Rotation
Force	Gravitational Force on the Center	Gravitational Force on the Center of Mass, External Body Force	Gravitational Force on the Center of Mass, External Body Force

2.2.1 Parabolic Equations

In the lumped mass method, rocks translational motion is controlled by conventional physics equations derived from Newton's law. In three-dimensional (3D) form, the location and velocity of the rock at each time interval are described by Equation 2-1 and Equation 2-2 (Stevens, 1998).

$$\begin{aligned}
 V_z &= \int_0^t -g dt = V_0 - g \cdot t, \\
 V_y &= \int_0^t a_y dt = V_{0y}, \\
 V_x &= \int_0^t a_x dt = V_{0x}
 \end{aligned}
 \tag{Equation 2-1}$$

$$\begin{aligned}
 z &= \int_0^t (V_0 - g \cdot t) dt = Z_0 + V_0 \cdot t - \frac{1}{2} g t^2, \\
 y &= \int_0^t V_{0y} dt = y_0 + V_{0y} \cdot t, \\
 x &= \int_0^t V_{0x} dt = x_0 + V_{0x} \cdot t,
 \end{aligned}
 \tag{Equation 2-2}$$

2.2.2 Rock-ground Interaction Mechanics

In the lumped mass model, the rock is considered as a moving point, and its direction is affected by the alignment of the surface at each bounce. Dip and dip direction of the surface plane modify direction cosines of the rock after each bounce. Rock velocity is divided between three orthogonal directions (x, y, z). At the impact point, this vector is first transformed to tangential and normal components of the surface consisting of two

tangential components reflecting dip ($v_{t,x}$) and dip direction ($v_{t,y}$), and a normal component (v_n). In other words, rock velocity is transformed into the surface plane coordinate system and then back to the global coordinate system at each bounce. Figure 2-2 illustrates vector components of rock velocity before bounce as well as the plane coordinate system (Lan et al., 2007).

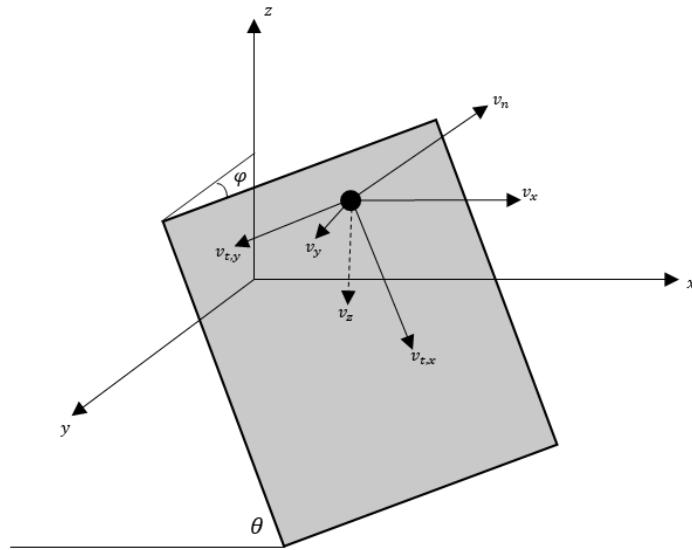


Figure 2-2 Illustration of velocity vectors transformation according to plane dip and trend (Modified from Lan et al., 2007).

Equations Equation 2-3 to Equation 2-8 show computations required for the rebound velocity calculation at the impact point of rock and surface (Stevens, 1998).

$$v_n = v_{z,b} \cdot \cos(\theta) \cdot \cos(\varphi) - v_{x,b} \cdot \sin(\theta) - v_{y,b} \cdot \sin(\varphi) \quad \text{Equation 2-3}$$

$$v_{t,x} = v_{z,b} \cdot \sin(\theta) \cdot \cos(\varphi) + v_{x,b} \cdot \cos(\theta) \quad \text{Equation 2-4}$$

$$v_{t,y} = v_{z,b} \cdot \sin(\varphi) \cdot \cos(\theta) + v_{y,b} \cdot \cos(\varphi) \quad \text{Equation 2-5}$$

$$v_{z,a} = v_{t,x} \cdot \sin(\theta) + v_{t,y} \cdot \sin(\varphi) - v_n \cdot \cos(\theta) \cdot \cos(\varphi) \quad \text{Equation 2-6}$$

$$v_{y,a} = v_{t,y} \cdot \cos(\varphi) + v_n \cdot \sin(\theta) \cdot \cos(\varphi) \quad \text{Equation 2-7}$$

$$v_{x,a} = v_{t,x} \cdot \cos(\theta) + v_n \cdot \sin(\varphi) \cdot \cos(\theta) \quad \text{Equation 2-8}$$

where θ is the dip of the surface and φ is the plane dip direction. The notation ‘b’ indicates velocity components before impact, while the notation ‘a’ represents rebound velocity components.

2.2.3 Restitution Coefficients

One relatively easy way to account for the energy loss at each bounce is to consider tangential and normal coefficients of restitution (COR). A general definition for restitution coefficients can be the ratio between the rebound and the incident velocity of the rock at the contact point of the rock and surface. These coefficients are defined in two tangential and normal directions (Asteriou et al., 2012) as shown by Figure 2-3.

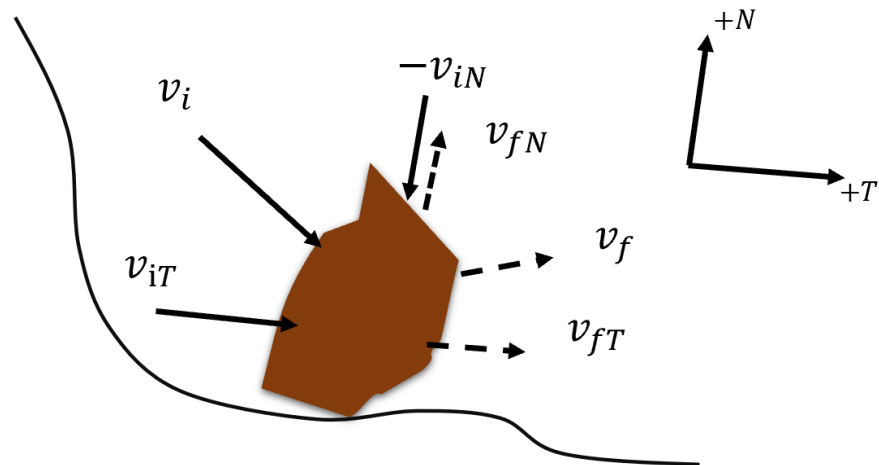


Figure 2-3 Illustration of how restitution coefficients affect rock translational velocity (modified from Wyllie, 2014).

The magnitude of the ball velocity is controlled by two restitution coefficients when impact occurs. Inelastic compression of slope materials and frictional forces influence normal and tangential coefficients. Restitution coefficients can be computed by Equation 2-9 and Equation 2-10 (Wyllie, 2014a).

$$R_N = -\frac{\text{Final normal velocity, } v_{fN}}{\text{Impact normal velocity, } v_{iN}} \quad \text{Equation 2-9}$$

$$R_T = \frac{\text{Final tangential velocity, } v_{fT}}{\text{Impact tangential velocity, } v_{iT}} \quad \text{Equation 2-10}$$

2.3 Rockfall Experimental Analysis

To prevent high-cost computations and unreliable input data for large field investigations, CORs are developed for each rock and ground surface material based upon small scale experiments. In such trial rockfall tests, incident and rebound velocities are

measured for similar surfaces and rock types as the field lithology. Although scale effect is the most important factor for avoiding rockfall laboratory experiments, valuable data has become available from such studies. Hu et al., (2018) conducted a small-scale experiment to find factors influencing the lateral dispersion of rocks. A combined model test-bench was constructed as part of their research where rocks were artificially manufactured. They chose various shapes, weights, and release heights for rock blocks throughout their tests. Finally, an empirical correlation for the lateral dispersion of cubic blocks was developed. It should be noted that most small-scale experimental research has been conducted to find those factors that influence restitution coefficients.

Full-scale experimental analysis intends to manipulate those parameters affecting rockfall trajectory assessments by monitoring real rockfall events in a pre-investigated area, with known rockfall source locations and rock features. Caviezel et al. (2019) performed a full-scale rockfall experiment to highlight the complexity of the rock-ground interaction. Implementing remote-sensing and measurement sensors, rockfall trajectories were captured along the designated area. Bounce heights and lengths, rock spin, and the change in acceleration at the point of contact were recorded. They concluded that CORs are incapable of representing the practical rock-surface interaction in soils. For reliable estimation of this interaction, rock geometry, surface roughness and soil scarring should be considered.

In another approach to account for the variability of the restitution coefficients, Bourrier et al., (2009) conducted a stochastic analysis to find the minimum field data to generate reliable coefficients. They performed a full-scale rockfall experiment in Foret Communale de Vaujany in France. A natural slope was considered as the rockfall path and,

utilizing eight high-speed cameras and laser technologies, they found rock stopping points and impact locations. Due to limitations on camera resolution, only translational movements of rocks were studied. They also implemented Rockyfor3D for modeling rockfall experiments. Characteristics of this software are described in section 0. They found acceptable agreement between results from the simulation model they developed and experimental results measured in the field in terms of rock rebound velocities.

2.4 Probabilistic Modelling

At first glance, rockfalls look like a relatively simple mechanical process. For a given starting point, topography of the slope and benches, energy lost at each impact, and the effect of friction throughout the path should be enough to predict rock velocity throughout the fall and also anticipate runout zone; however, in finding each of these factors, some restrictions cause uncertainty and result in error accumulation. Additionally, there are more contributing factors affecting rockfall trajectory such as shape and geometry of the rock boulder, as well as mechanical properties of the surface and the rock (Ritchie, 1963).

Identifying the exact location of a rockfall source is very difficult in the field. New advancements in drone and photogrammetry technologies make finding detailed 3D terrain models of the rockfall path more practical, although roughness and mechanical properties of different sections of the topography are still challenging to obtain. Due to these and other limitations, accurate estimation of energy loss in each bounce is not possible. Moreover, according to experimental findings, any minor changes to initial location coordinates of the rock can result in a wide range of discrepancies in estimated rock runout zones (Lan, Li, & Wu, 2015). To account for uncertainties related to rockfall sources, Scioldo, (1991)

proposed that at each starting point, several rockfall tests should be conducted at different angles.

Due to all of these uncertainties, probabilistic (stochastic) modelling is recommended to be used to account for scattered rockfall trajectories. This can happen perfectly in simulation programs where the capability to perform statistical analysis along with random selection of parameters exists.

2.5 Computer Simulation

Despite valuable data becoming available from full-scale rockfall experiments, they are costly and difficult to perform. Hence, a wide variety of research studies were conducted to develop different rockfall simulation techniques. The use of computer programs to analyze rockfalls started in 1960. Progressively, two and three-dimensional simulations have been used in risk assessment and hazard mitigation of rockfalls (Agliardi and Crosta, 2003; Bourrier et al., 2009; Dorren et al., 2011; Lambert and Coll, 2014; Lan, et al., 2007; Schweizer et al., 2013; Volkwein et al. 2011). In computer simulations, spatial information can be obtained from stopping points, velocities, bounce heights and lengths, and lateral dispersion of the rock which can be extremely helpful when designing protective measures where there is a lack of historical data (Peng, 2000).

Rockfall trajectory simulations can be categorized based on the scope of analysis, the kinematic method used for rock-surface interaction, and estimation procedures employed. Piteau and Clayton, (1976) developed a two-dimensional (2D) simple computer program to simulate rockfalls. Since then, several 2D and 3D programs have been developed to generate more reliable results for rockfall trajectory assessments. Some of the early

attempts are summarized by Guzzetti et al., (2002). Two-dimensional simulations provide a quick and handy hazard estimation. They use different probabilistic methods to account for any shortcomings; however, they cannot consider the lateral dispersion of rock. Although a 3D simulation is much closer to reality than a 2D analysis, a 3D terrain model is expensive to acquire, especially considering slope profiles can easily be made for a 2D analysis.

As stated previously, lumped mass, rigid sphere (hybrid), and complex rigid body are the three kinematical approaches used in trajectory modelling with the lumped mass approach being most popular due to its simplicity and quickness in completing computations. The weakness of this method is that rock rotation is overlooked, and rolling cannot be physically considered in the modeling. Although, the rigid sphere model solves this issue, considering a spherical shape for the rock overestimates runout zones as the sphere keeps rolling on an inclined plane (Schweizer et al., 2013).. Complex rigid body method allows for complete dynamic and physical modelling of the rock motion, although higher computation time is required and many more input parameters and specifications are needed both for the rock shape and for surface properties. Giving consideration for inconsistent input data, large discrepancies might be generated in results leading to more difficult hazard estimation at large scale (Pfeiffer & Higgins, 1990).

The analysis type in physical modelling of rockfalls is essential in achieving reliable outcomes in an effective computational time. Finite element (FE) and discrete element (DE) methods allow for stress and displacement analysis and plasticity in rock-surface interactions and the rigid body method considers the rock motion significant enough to ignore micro-displacements of the rock and/or surface at each bounce. This method always

uses semi-empirical relations along with dynamic equations for simulations. Additionally, probabilistic analysis plays a critical role in this method, which is used along with several statistical methods in most simulation programs (Schweizer et al., 2013).

Next, a high-level review of rockfall modelling programs is presented on several recently developed software. It is based on those modelling characteristics just described.

2.5.1 STONE and Hy-STONE

Attempting to address limitations of rockfall software in handling large areas, the STONE program was designed to allow the user to study hundreds of square kilometers where no detailed information is available. Coded in ANSI C language, the STONE program is a 3D rockfall simulator at the regional and local scales. It requires DTM as the terrain input data in raster format both for the rockfall area and source locations in which each cell represents a rockfall starting point. The restitution coefficients and dynamic friction coefficient should be given in a grid format. Also, a text file should be provided containing initial and controlling parameters such as starting velocity, minimum velocity, and fly/roll transition thresholds. A lumped mass approach was employed in a discrete time-interval modelling method. The triangular terrain model was also derived from DTM where trajectories were calculated.

The start of the rockfall in STONE software is a horizontal motion along the steepest slope. The rock then travels a parabolic trajectory, and the elevation of the boulder is monitored at each time interval and compared to the DTM elevation for detecting impact points. Once contact is detected, velocities of the rock will be updated based on the incoming direction of the rock and the tangential and normal restitution coefficients to

account for loss of energy. This process continues until frictional forces are higher than reflection forces. In this situation, rolling occurs, which is modelled simply by only applying a drag force in the opposite direction of rock motion.

Once the rock stops and the analysis is finished, outputs including the total number of rockfall trajectories, and the highest velocities and bounce heights will be recorded in raster image format (Figure 2-4).

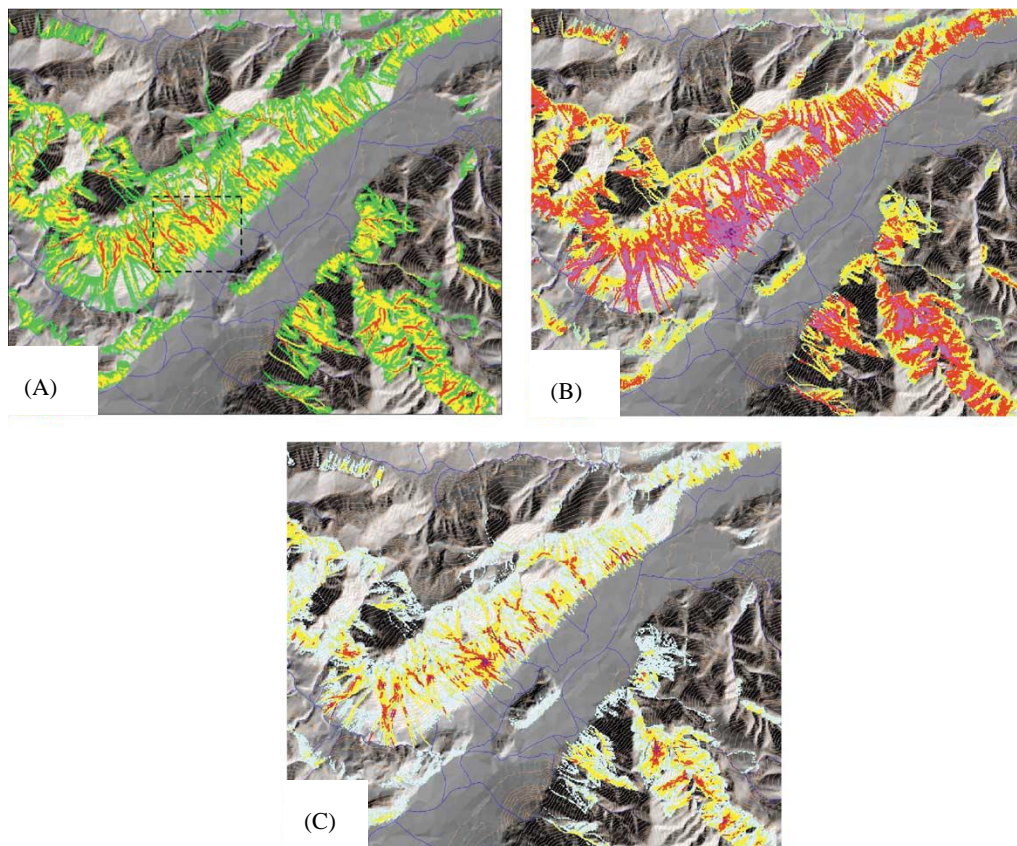


Figure 2-4 STONE raster outputs showing (A) number of rockfall trajectories, (B) Maximum rockfall velocities ranging from 50 km.h^{-1} (green) to more than 300 km.h^{-1} (red), (C) Maximum height trajectories above ground ranging from 5m to 100m.

In addition to the output being offered in various formats, it utilizes an approach to account for uncertainties in input data, especially for big areas. A user-defined variation of

input data can be specified. Moreover, during each run, the rockfall source, rebound coefficients, dynamic friction coefficient will be selected within a specified range.

The performance of STONE software was evaluated against two other rockfall software that became available at about the same time. They are Rocscience's Rockfall and CRSP. A simple slope with an angle of 50° was tested in both programs. The three simulators each gave a different stopping point for the rock. This was inevitable; however, there were similarities between STONE and Rockfall in rebound velocities and heights for the upper part of the slope, while STONE and CRSP were close in the lower part of the slope. The main difference in the three programs that caused differences in stopping points was in the method used to switch from bouncing to rolling.

The STONE program was also evaluated in another case study in which a synthetic 3D topography was used and the rockfall was mostly directed towards the concave area due to topographical effects. Finally, STONE was examined using real topography from an alpine valley that has an area of 1450 km^2 . The DTM utilized had a resolution of 20 meters. Based on available geology and survey information, input data were selected. After running over 400 rockfall tests, concave areas and channels were clearly identifiable showing the rock path when falling. Additionally, high values for rock velocity and bouncing heights were recorded near large cliffs.

In later developments of the program, a hybrid method was used instead of the lumped mass model. Probabilistic methods and capabilities were upgraded, along with a new feature by which the effect of catch nets could be considered in the analysis. Outcomes were also extended to include maximum runout zones, type of rock motion, and impact locations. With addition of the hybrid method to the existing program, the name changed

to Hy-STONE to highlight the difference in the rock kinematic model (Guzzetti et al., 2002).

2.5.2 Rockfall Analyst

In this research, 3D rockfall modelling was carried out based on a GIS database. Rockfall Analyst (RA) is an extension of the ArcGIS software developed by Environmental Systems Research Institute, Inc. (ESRI). RA takes both raster (GRID) and vector data as well as mechanical properties of the terrain. Rockfall frequency, bouncing height, and kinetic energy are computed along with an assessment of barriers' effectiveness in rockfall hazard mitigation. In general, two types of analysis can be conducted by RA: rockfall trajectory simulation and raster modelling for the spatial distribution of rockfalls. As this software utilizes the GIS interface, the rockfall frequency and predicted rockfall runout zones are estimated using geostatistical methods. Similar to STONE, the digital elevation model is used as a terrain model and bouncing, rolling, and sliding stages are calculated based on each cell plane direction. As shown in Figure 2-5, the dip and dip direction angles were defined for a 3×3 or 5×5 neighborhood setting and their mean value is incorporated in RA for a meaningful representation of real topography and to generate plane surfaces from DEM cells.

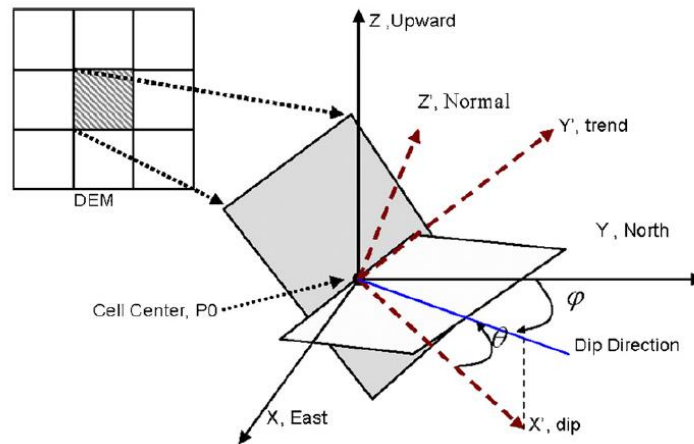


Figure 2-5 Definition of the plane coordinate system associated with neighboring cells.

Kinematical modelling of rockfalls was performed in a time-interval approach controlled by cell size and particle velocity. Impact points between the rock and plane surfaces were detected by inside/outside tests in such a way that once the rock is detected under the plane the impact has occurred and then either a quadratic equation will be solved for a parabolic and line intersection or line and plane intersection as the time intervals are very small. Once the impact point is found, the bouncing direction is calculated based on geometric optics and according to restitution coefficients. After the projectile motion of the rock has reached the minimum threshold for rock velocity, rolling or sliding starts along the steepest path of the slope.

In addition to trajectory simulation, RA utilizes geostatistical methods to overcome the uncertainty of input data. For instance, even though some information becomes available for a portion of cells, with geostatistical autocorrelation other surrounding cells gain similar properties. Kriging, a tool often implemented in mineral resource estimation, is used in RA along with GIS inverse distance weighted (IDW) and mathematical and statistical methods to identify properties of unknown cells. Several rockfall tests can be simulated based on

seed values for source location, initial velocities, and surface properties such as slope, roughness, land use, geology, vegetation cover, and structure.

The performance of the RA GIS extension was evaluated by the Canadian Pacific Railway in the Cascade subdivision. DEM data was collected from aerial LIDAR technology with 1_m resolution and 600 rockfall events were studied from 1940 to 2003 to find possible source locations of rockfalls and to determine different combinations of coefficients for incorporation in simulations. Seven sets of properties were defined for the topography and four source locations were selected at different distances from the railway. Nearly 1,000 rockfall tests were simulated for various source locations and runout zones for each of them were evaluated. According to simulation results, most rocks falling from the four major source locations would reach the vicinity of railway tracks. This is consistent with field observations and historical data.

Trajectory results showed that some portion of the rocks would bounce over the railway track and reach the river as can be seen in Figure 2-6. In the next phase of the project and to address the rockfall hazard in Source 1, a concrete wall was designed and trajectories were re-analyzed considering the concrete barrier. A 5 m high concrete wall was selected for simulation. As shown in Figure 2-7, only one rock reached over the barrier. Rockfall Analyst showed reliable results in a quick and probabilistic approach where the effectiveness of protection measures could also be evaluated (Lan et al., 2007).

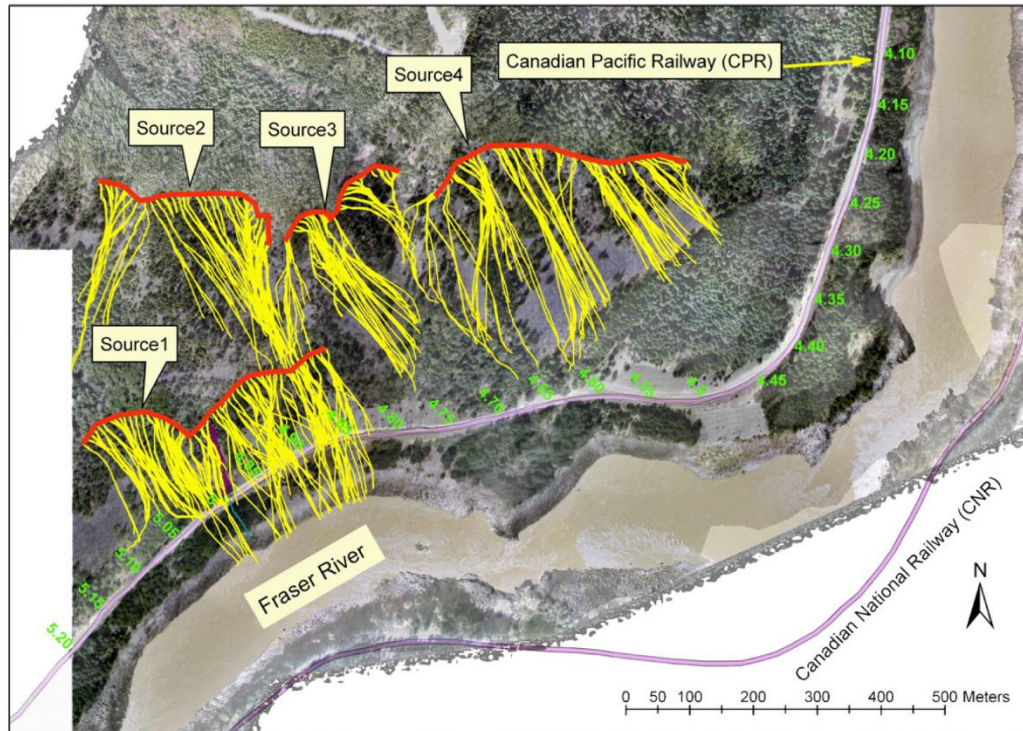


Figure 2-6 Trajectories for four source areas with Sources 1 and 2 exhibiting the highest hazard to railway tracks.

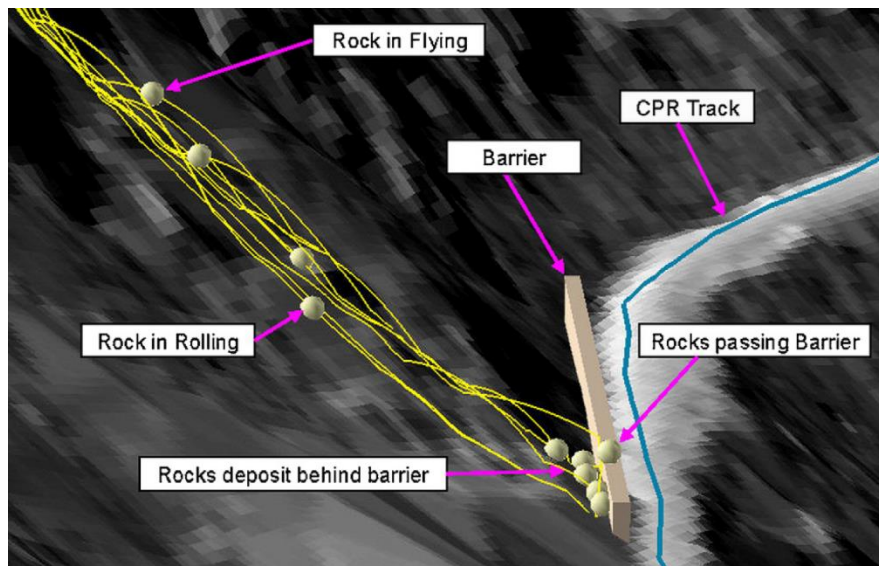


Figure 2-7 Rockfall trajectories considering a concrete barrier in their path to the railway track.

2.5.3 *CRSP3D*

Unlike other commercial rockfall simulators, this program uses discrete element method (DEM) for rock-slope interactions along with physical motion equations. It is capable of simulating all aspects of rockfall trajectory such as flying, bouncing, rolling, sliding, and damping. Previously developed in a 2D environment with conventional physical methods for rockfall modelling, CRSP3D is an upgrade of CRSP, which no longer works with semi-empirical relations but benefits from fundamental physical and computational modelling. In such an environment, a linear elastic behavior is defined for impacts of rock and slope in which a damping ratio is also defined for settling down rebounds (similar to the tangential restitution coefficient). CRSP takes a hardness coefficient as the indicator for surface properties and a function of the coefficient of restitution to account for collision elasticity (Jones et al., 2000). The 3D version of CRSP was used in simulating rockfall trajectories in a case study at Gunung Batu, Indonesia (Nugraha et al., 2017).

The very first stage of working with CRSP3D is calibration. A controlled rockfall test is often used for this purpose. Calibrating parameters are geometry, roughness, hardness/stiffness of slopes, and suitable rock forms.

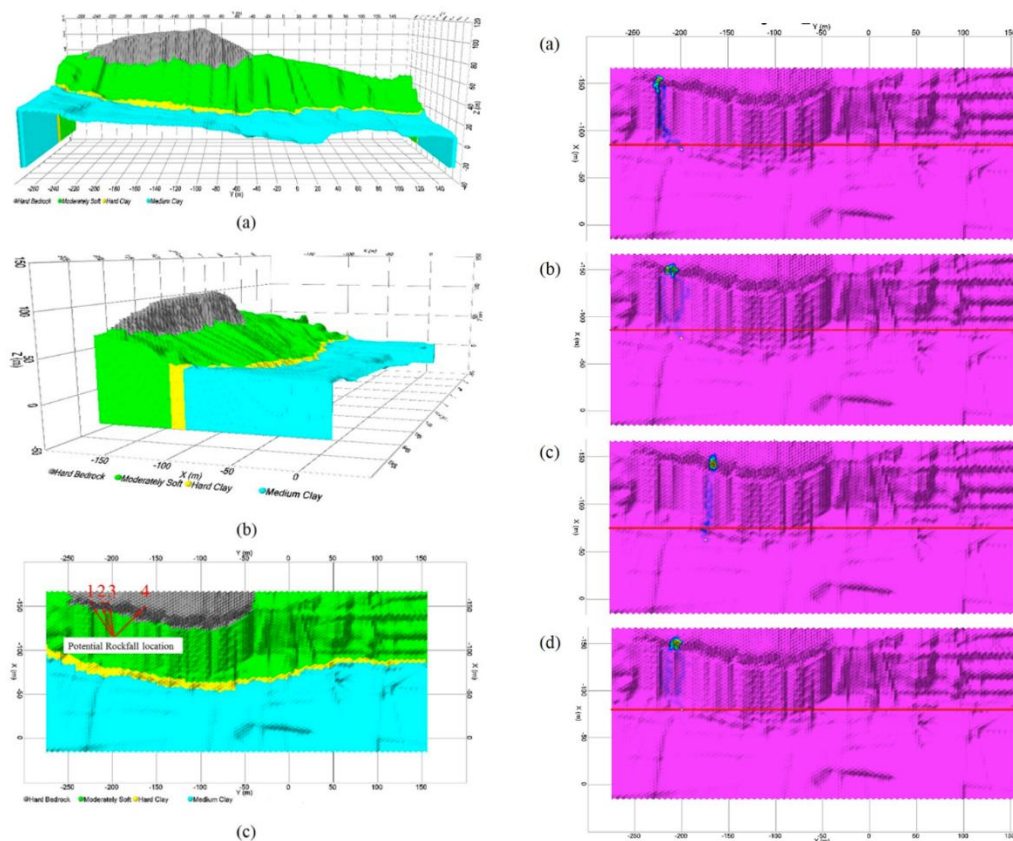


Figure 2-8 CRSP3D output: rockfall source locations and trajectories (Nugraha et al., 2017).

Based on field observations, four source locations were identified where trajectory simulations show that runout zones would reach the border of the slope and road (red line) and some of them even go further into residential areas (Figure 2-8).

2.5.4 Rockyfor3D

Incorporating physical modelling equations along with stochastic methods, Rockyfor3D simulates a process-based rockfall trajectory analysis on different scales. While accounting for free fall, bouncing, and rolling as well as short rebounds, Rockyfor3D does not consider sliding in the trajectory analysis. It takes ten ESRI ASCII grid format raster files with 2 m or 10 m resolution. Inputs include a DEM, a raster map with rock

density for each cell, three raster maps including block height, width, and length for each source location, another raster map defining the rock shape with four general options (rectangular block, ellipsoidal block, spherical block, and disc-shaped block), three raster maps for defining slope surface roughness, and finally a raster map for underground condition representation with eight options for restitution coefficients.

One of the unique features of Rockyfor3D is the capability of incorporating vegetation and forests into the trajectory analysis. It can do such by either taking the coordinates of each tree in the area or representing the vegetation by four raster maps representing the number of stems per hectare, the mean stem diameter at breast height (DBH) per cell, the standard deviation of DBH in each cell, and the mean percentage of coniferous trees within each cell. Additionally, rockfall nets can be considered in the analysis by three raster files giving energy absorption capacity and height of nets to the model where the total number of rocks caught in nets and their kinetic energy will be calculated.

The performance of the program was evaluated in a real case study in the Forêt Communale de Vaujany in France. A set of full-scale rockfall tests were performed in the area where the mean gradient of the slope was 38°. In this case study, due to the very large experimental area and low resolution of high-speed cameras, rotational velocity was not monitored in rockfall tests. The DEM of the site was generated utilizing inverse distance-weighted interpolation and a detailed topographical survey conducted by a laser distance meter and a compass. The surface roughness is represented in three categories that control rebound coefficients. The bouncing computation in Rockyfor3D is different from classical physical modelling in such a way that three coefficients were defined for tangential, normal, and rotational velocities. As Equation 2-11 illustrates, rebound tangential velocity

is given as an example of the proposed model. The tangential velocity after the bounce is the summation of the incident tangential, normal, and rotational velocities according to their coefficients (a_1, a_2, a_3) that are defined according to the normal probability distribution functions calibrated from laboratory experiments.

$$V_t^{out} = a_1 V_t^{in} + a_2 V_n^{in} + a_3 \omega_n^{in} \quad \text{Equation 2-11}$$

In addition to rebound modelling, the lateral dispersion of the rock was also considered in these simulations. The cell aspect plays a determinative role in this calculation, which refers to the steepest slope direction of the cell among its neighboring ones. The boulder can deviate from 0° to 22.5° or 22.5° to 45° , or 45° to 50° from its original direction distributed based on the probability of occurrence of each scenario (Figure 2-9). These scenarios vary when rock travels down slope or up slope.

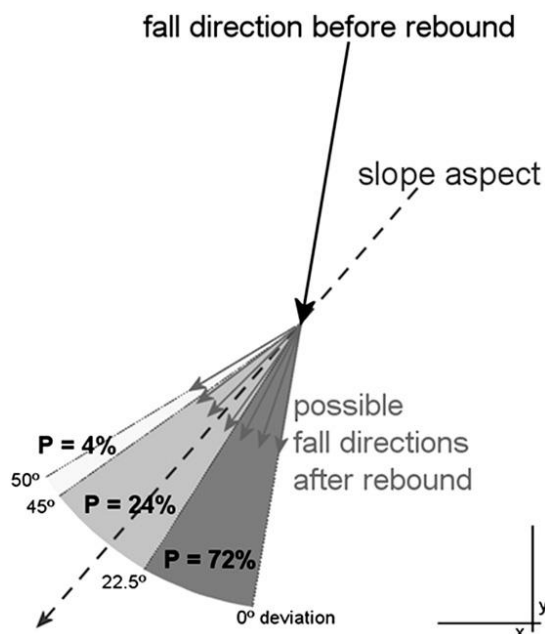


Figure 2-9 Possible lateral dispersion of the rock when impacting the slope.

Finally, more than 10,000 rockfall simulations were carried out and compared with experimental tests in terms of passing heights, translational kinetic energies, velocities, spatial patterns of trajectories, passing frequencies per cell, and stopping points. It was concluded that simulation outcomes were in acceptable agreement with experimental results; however, simulations overestimated runout zones in comparison with reality. The rebound model was also found to be effective in predicting correct rebound velocities on hard surfaces; however, Rockyfor3D is not designed for rock-surface interactions in fine soils (Bourrier et al., 2009).

2.5.5 RAMMS:: ROCKFALL MODULE

A rigid body kinetic approach was incorporated in developing this robust 3D rockfall trajectory model. Primarily designed for avalanches and debris flow, the outstanding benefit of RAMMS (Rapid Mass Movements) is the capability to consider irregular rock shapes in dynamic motion analysis. Starting from the terrain model, RAMMS is designed to take representing parameters for surface hardness, scree content, soil cover, and vegetation in DEM formats (Schweizer et al., 2013). The rock is modeled as an arbitrary convex polyhedral originating from the morphology of the rock in a multibody and non-smooth contact dynamics that is an unbreakable 3D body. Additionally, this program takes advantage of a friction law designed by the developer (WSL Institute for Snow and Avalanche Research SLF) to account for the scarring behavior of the rock. This allows for considering a small amount of sliding at each rock bounce as shown in Figure 2-10. The forest can also be considered by a drag force.

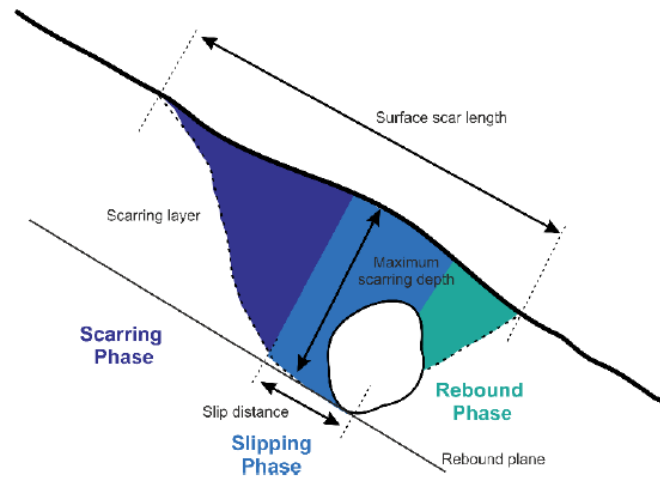


Figure 2-10 Illustration of the scarring phenomena (Modified from Dorf, 2019).

The concept of tackling the rock-ground interaction in RAMMS:: ROCKFALL is different from the coefficients of restitution (COR) method. Unlike conventional methods in which each impact is assumed as a single-point, in this program the terrain is assumed to have two non-deformable and hard-contact areas. This method can account for rock penetration into the soil until the maximum scar depth is reached. This depth was empirically correlated to soil and rock strength and incoming velocity. This is called the scarring phase which is followed by sliding and rebound phases. Accordingly, instead of implementing a one-to-one relation between normal and tangential forces and considering the rock-surface interaction as a single incident that only results in a rebound, more detailed computations are considered to simulate the practical behavior of the rock.

A detailed review of concepts and theoretical formulations of the RAMMS program is beyond the scope of this research, yet a review is provided on its practical performance in simulating the rockfall trajectory. “Chant Sura” located near Davos, Switzerland was selected as the experimental site in which slope angles vary from 40-80°. Fixed high-speed

resolution cameras and moving sensors installed on rocks were used to track rock motion and energy along the falling path. Rock blocks were built from reinforced concrete in two shapes to represent worst-case scenarios in both runout zones along with the dip stream direction and lateral dispersion. Hence, cubic and platy shapes were selected and released using a hydraulic platform at the source location. The stopping point of rocks was also measured with 5 cm discrepancy. In addition to measuring devices, high-resolution digital surface models were also gathered before and after experiments with drones to locate ground scars and rough trajectory tracking in virgin terrain. Initiating from a single starting point, different rock masses and shapes were selected for 163 rockfall tests during a 2-year period. Model calibration showed good agreement between simulations and experiments in which the scar drag model was also proved to be simple and reliable in modelling (Dorf, 2019). Figure 2-11 RAMMS 3D outcome overview shows an outcome overview of RAMMS 3D in trajectory simulation with 3D trajectories and 2D profiles given for different rock shapes. The velocity of the rock is also plotted in the raster format

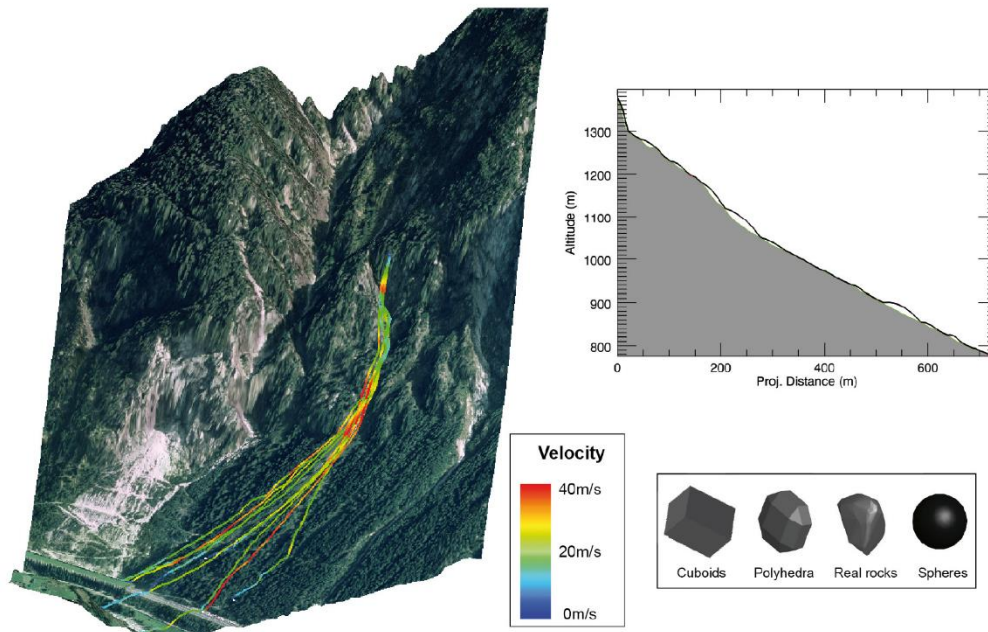


Figure 2-11 RAMMS 3D outcome overview (Schweizer et al., 2013).

2.6 Summary

In this research, the experienced gained from analyzing those programs that were mentioned was used to develop a 3D computer program named Rock PathFinder (RPF3D) for rockfall trajectory simulation. Existing rockfall simulation programs provide a high-level analysis of rockfall trajectories given required input parameters, which is hard to obtain safely and accurately. Furthermore, those programs are incapable of generating hazard maps for rockfall runout zones. To address these limitations, RPF3D is designed to provide a “Rock Trace Map” from trajectory simulation. In a rockfall incident, the trace of the rock’s trajectory on the surface can be visualized in a 3D format.

Key characteristics of programs reviewed in this chapter are summarized in Table 2-2 along with RPF3D features. The level of kinetical method used, terrain model resolution

compatibility, input data complexity, and the skill set required to run rockfall simulations are compared.

Table 2-2 An overview of the current rockfall simulation programs and RPF3D.

Program	Kinetic approach	Terrain Model Resolution	Outcome	Input data complexity	Skill level needed
STONE	Lumped mass	Low	Number of trajectories, Maximum rockfall velocities, Maximum height trajectories	Medium	Medium
Rockfall Analyst	Lumped mass	Low	Rockfall trajectories, bounce height-length, runout zones	Medium	Medium
CRSP	FEM	Low	Rockfall trajectories	High	High
Rockyfor3D	Rigid body	Medium	Passing heights, Translational kinetic energies, Velocities, Spatial patterns of trajectories, Passing frequencies per cell, stopping points.	High	High
RAMMS	Complex rigid body	Low	Velocities, Trajectories, Stopping points	High	High
RPF3D	Lumped mass	High	Trace map, Trajectories, Velocities, Bounce height-lengths, Stopping points	Low	Low

RPF3D maintains a relatively simple analysis scope along with powerful techniques for trajectory simulation. The program's algorithms and experimental calibration are expressed carefully in Chapters 3 and 4.

CHAPTER 3 : PROGRAM DEVELOPMENT

As mentioned in Chapter 2, rockfall modeling programs are in a high-demand by industries such as road construction and open-pit mining. Although available programs provide high-level physical and stochastic analysis of rockfall trajectories, controversy exists over whether they can provide a reliable estimation of rockfall runout zones. In open-pit mines where input parameters are limited and rate of face advance is fast, effective analysis of runout zones is critical; however, most rockfall modeling programs require extensive field data and, more importantly, they are not designed to provide hazard maps for use in open-pit mines. Therefore, the main objective of this thesis is to fill this gap by developing RPF3D to simulate rockfall trajectories for open-pit mines and identify potential rockfall runout areas. In this chapter, a comprehensive overview of the program is given including discussion of assumptions, limitations, and a step-by-step analysis of the program's algorithms.

RPF3D is designed specifically for conditions faced in open-pit mining and to provide a quick and reliable tool for rockfall hazard risk assessment. Table 3-1 summarizes assumptions made in developing the program.

Table 3-1 General assumptions of RPF3D.

Model	Scope of Analysis	Kinetic analysis type	Mechanisms Allows	Impact- modeling
Assumptions	Three-dimensional	Lumped mass (vector)	Falling and Bouncing	Semi-empirical - elastic

3.1 RPF3D Input Parameters

One of the most challenging stages in rockfall trajectory modeling is obtaining input data. Depending on the type of modeling or the scope of analysis, various physical,

mechanical, and geological parameters should be collected from the project site. These might include existing field topography (within acceptable standards for resolution); rock mass properties for determining frictional forces and energy loss at each rock-surface contact; an estimation of rock size, shape, and weight; and the initial location and velocity of the rock. In RPF3D, rock-surface energy loss is considered using a semi-empirical model that incorporates coefficients of restitution (CORs). Since a lumped mass model is used, only the rock's initial location and velocity are required.

In current rockfall programs, probabilistic modeling of rockfall is most often practiced using random values for CORs, source locations, and initial velocities to address shortcomings from surface geometry and geological data, and uncertainties about rockfall risk on highwalls and slopes. In RPF3D, however, the surface topography can be modeled with high accuracy in 3D as there is no limitation to the model size (number of mesh).

Similar to other rockfall programs, a discrete time-interval approach is used in RPF3D where the desired time-step is given by the user. Another important parameter that is essential for computations is the impact threshold. This is defined as a circular area such that if the absolute value of the distance between rock and surface falls below the radius of this area, impact is detected. The smaller this threshold is, the more accurate the impact point is captured. This parameter can also be defined by the user. Default time-steps and impact thresholds for the program are 0.1 milliseconds and 5 cm for large-scale terrain models (*i.e.*, mesh elements numbering more than 1 million).

3.2 RPF3D Terrain Model

Various terrain formats are implemented by existing rockfall programs including the digital terrain model (DTM) that has various formats such as point files (dxf, csv, txt, xyz), raster altitude files (dem, asc), mesh files (stl, ply, 3ds), and raster images (png, tif, jpeg). According to the settings of each format, different methods are available for rendering such files for visualization. In rockfall trajectory simulation, the terrain model should be represented as a set of planes with known dip and dip direction to allow for optic geometrical equations to determine direction of rock motion at each bounce. The process of making such planes from a given topography format is called triangulation.

DEMs are the most prevalent formats composed of two-dimensional array cells (x, y) in which each cell is associated with an elevation value. The main problem with this format is that the triangulation process is performed by taking the average of neighboring cells, which causes some inaccuracies in rock-surface impact modeling. The stereo-lithography (STL) format files, however, represent the topography as a set of triangles along with their vertices and normal vectors. Figure 3-1 shows input data for each triangle in an STL file.

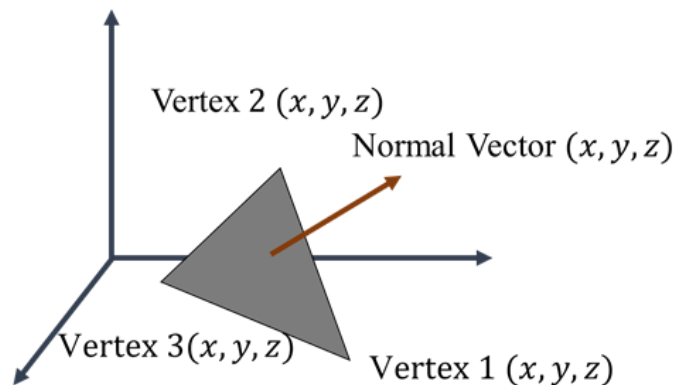


Figure 3-1 STL format geometry.

This format was initially developed in the manufacturing industry to represent geometries of real solids for rapid prototyping. Triangle meshes have shown an acceptable efficiency and flexibility in different applications and visualizations; however, polygons constructed with millions of triangles (*e.g.*, large open-pit mines topography) often require more extensive storage and long processing time (Szilvási-Nagy & Mátyási, 2003). This is one of the drawbacks of using STL format for rockfall trajectory simulation as not only the terrain is to be read and visualized, but also the correct triangle should be detected at each bounce. Hence, current rockfall programs lean towards DEM file formats or light STL files (*e.g.*, thousands of triangles) to provide faster computation of trajectories.

To enable rockfall modeling on heavy mesh files, Visualization Toolkit (VTK) was used in RPF3D development. VTK is an open-source python script package for 3D graphics, modeling, and image processing. This library is extensively used in biomedical research to visualize computed tomography (CT) scan figures that only come in STL format. VTK is suitable for storing various properties in one file without using much storage and computation time. For instance, VTK stores the information from an STL file in three connected data structures: coordinate points, triangles, and normal vectors. They are linked together and can be accessed individually resulting in faster computation. VTK then compresses all constructed data structures into one file (.vtk) that does not require much hard drive space. This file can contain different types of information. For example, in slope stability analysis of an open-pit mine, the slope's geometry, shear stress, normal stress, factor of safety, displacement, *etc.* can be stored in a single VTK file.

The VTK library also comes with free visualization software named Paraview. The VTK file can be visualized in Paraview and just by choosing the desired layer, different

information is available. This feature is extremely useful in sensitivity analysis and big projects where various types of results should be visualized on 3D mesh files.

Therefore, RPF3D was designed using different VTK algorithms to provide an optimized simulation and results visualization. RPF3D first transforms the STL topography to a VTP (VTK PolyData) format and stores each triangle as a cell with three vertices and a cell ID for further referencing. Normal vectors of these triangles will also be stored in a separate data structure for further use in kinetic equations. Proper CORs will then be assigned to different parts of the topography based on user preference and the output terrain will be saved as a VTP file for trajectory simulations. Figure 3-2 is an example of a VTP file visualization of an open-pit mine that shows the ID number of each triangle with a heat-map (cold to hot).

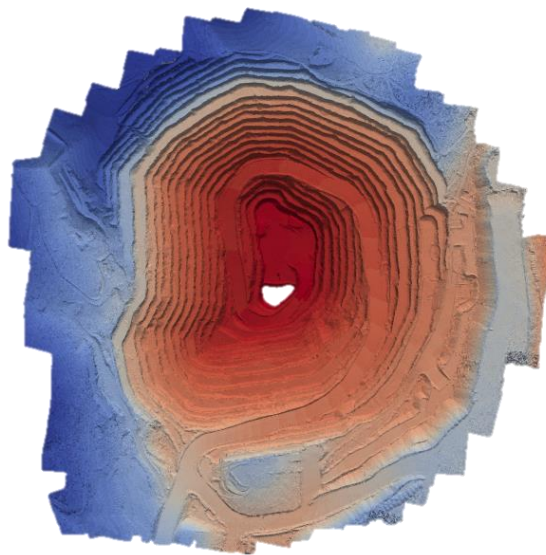


Figure 3-2 VTK poly data with id number for each triangle.

3.3 RPF3D Trajectory Modeling

After constructing the terrain model and obtaining the rock's initial location and velocity, the trajectory simulation starts using parabolic equations (Equation 2-1 and

Equation 2-2) along with optical geometry relations (Equation 2-3 to Equation 2-8) for rock motion and impact modeling. The impact detection algorithm searches among surface triangles as the rock moves and constantly measures the distance between the rock and nearby triangles. Once the distance becomes lower than the impact threshold, impact is detected, and velocities will be transformed to update the rock's direction after a bounce. Loss of energy at each bounce is also captured using normal and tangential restitution coefficients (Equation 3-1 to Equation 3-3).

$$v_{t,x,A} = v_{t,x,b} \cdot R_t \quad \text{Equation 3-1}$$

$$v_{t,y,A} = v_{t,y,b} \cdot R_t \quad \text{Equation 3-2}$$

$$v_{n,A} = v_{n,b} \cdot R_n \quad \text{Equation 3-3}$$

After each impact, the rock's initial location and velocity will be updated in the parabolic equation, and then the rock continues to move. After a certain number of iterations, and once the rock velocity becomes lower than a user-defined threshold, the program detects that the rock has stopped. Impact locations are recorded on the terrain model by highlighting each impacted triangle. The rock motion trace is also recorded in a separate format, and once the trajectory algorithm is finished, two VTP files will be generated. One of them is the terrain model with the rock trace on the surface; the other is the rock trajectory. They can be visualized in Paraview simultaneously to see a complete overview of the rockfall incident. Rock coordinates and velocity magnitude throughout the simulation are monitored and plotted versus horizontal distance allowing for 2D analysis of a rockfall trajectory. Figure 3-3 shows a sample of the output from a trajectory analysis conducted by RPF3D.

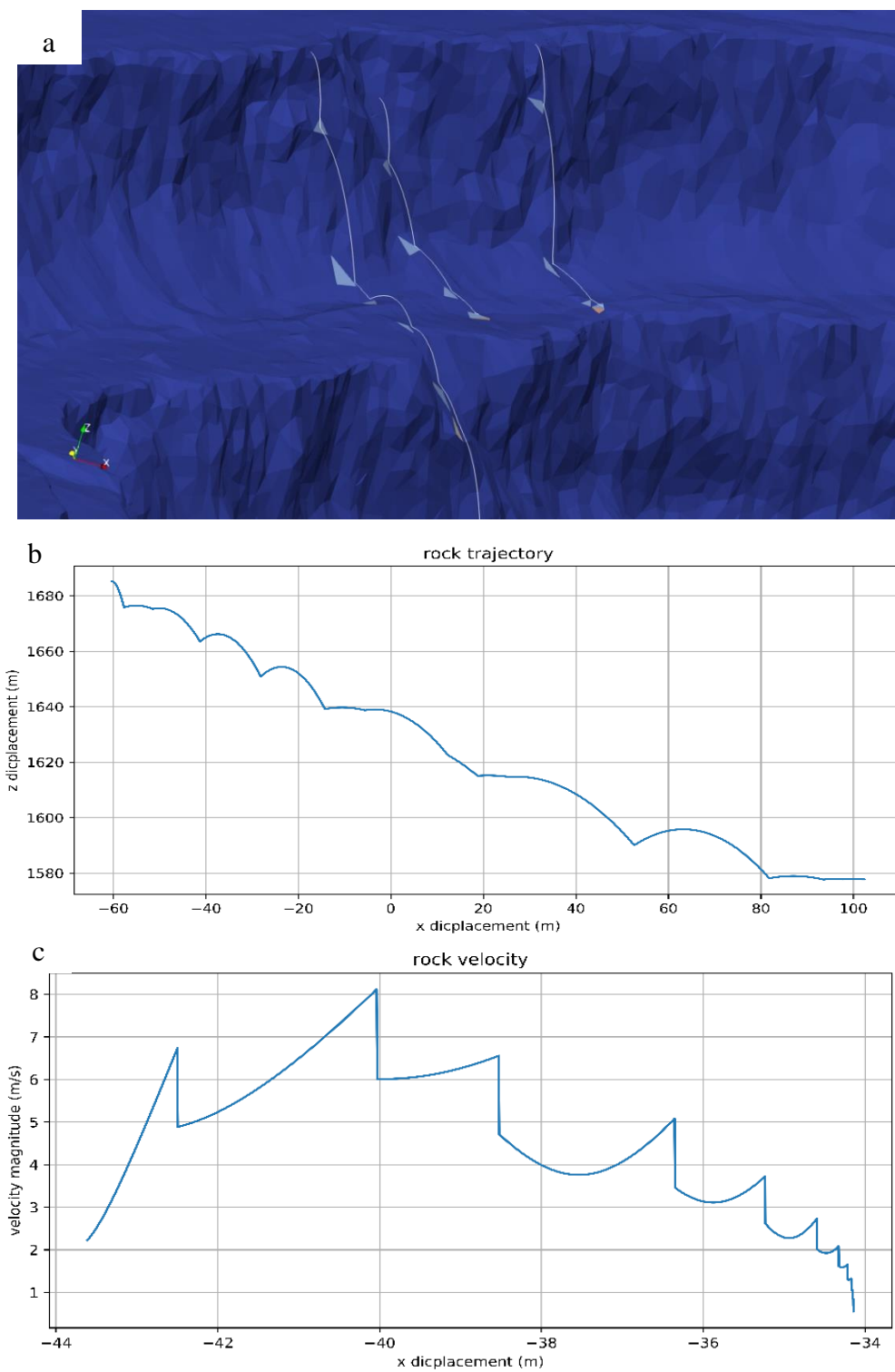


Figure 3-3 a) Sample trajectories and trace-map generated by RPF3D, b) 2D cross-section generated for one of the trajectories along with c) rock velocity throughout the trajectory.

The RPF3D algorithm is illustrated in Figure 3-4. Terrain model construction, rock motion, impact detection, and rock trace generation are the four major algorithms implemented in this program.

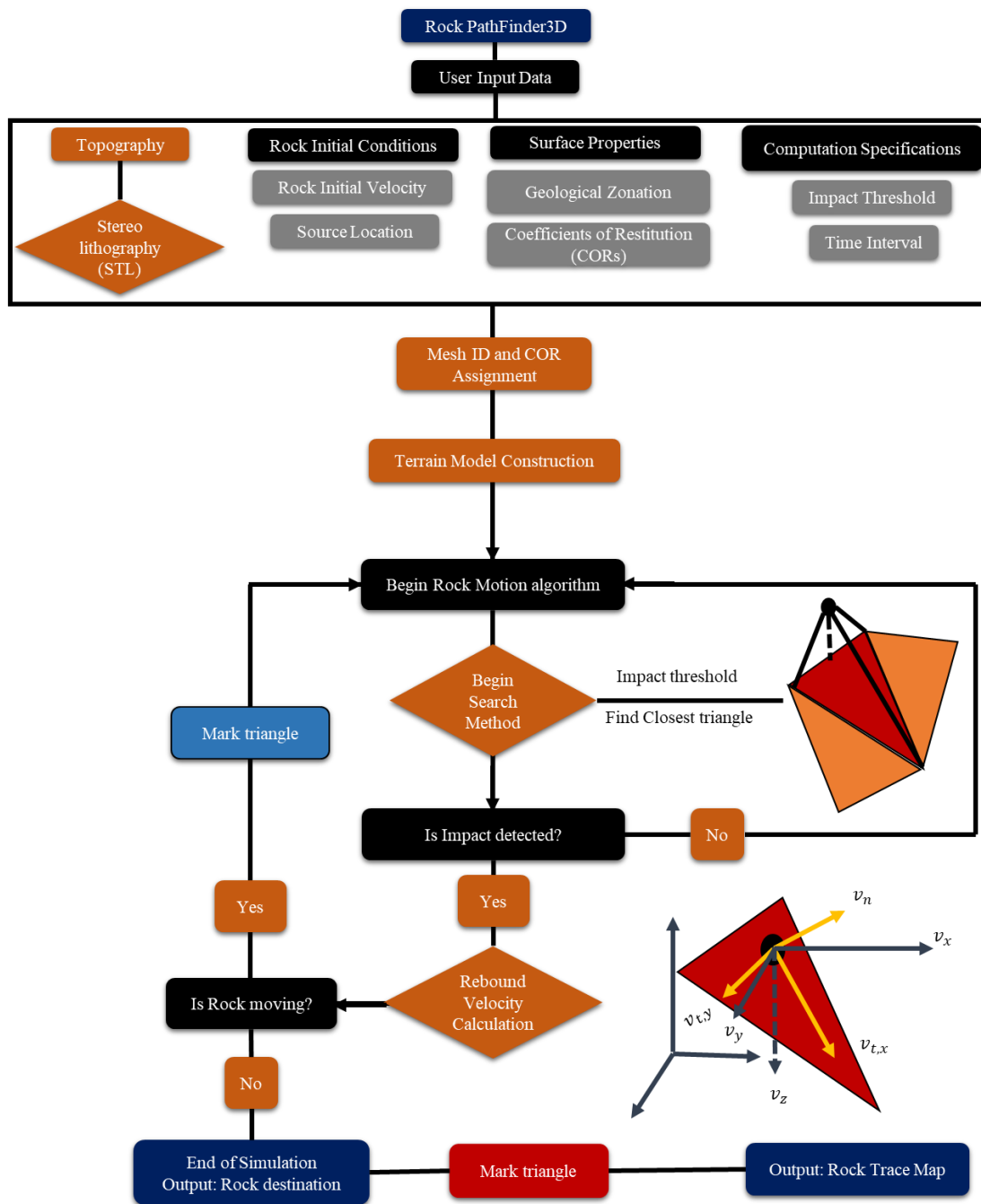


Figure 3-4 Code structure showing data input, terrain model, rock motion, impact detection, and stopping criterion algorithms.

3.4 RPF3D Impact Detection

In addition to the challenges involved with rendering large mesh files, searching and performing computations among them in each time-step is a very time-consuming task if performed primitively. Existing rockfall programs perform several trajectory simulations in less than a minute on DEM terrain models. This high speed of computation is a crucial factor in developing a rockfall program. Although RPF3D significantly improved the speed of reading heavy mesh files, trajectory simulations took much longer at the beginning of the program's development. Two major issues caused these very slow computations including searching among all the triangles and computing the point-plane distance at each time-step. In large topographies where the rock falls for several meters, the time-step must be small enough to allow for impact detection, which caused the number of computations and search attempts to increase drastically. Hence, there was a tremendous need for an optimized and advanced algorithm to overcome this issue.

For impact detection, the distance between the rock and each triangle in its vicinity is measured by the shortest distance formulas for point and plane. The VTK Cell Locator algorithm offers several methods for finding the closest point to a cell in a VTK poly data file. The most important feature of these methods is the optimized search method in which the program only looks for triangles within a limited sphere around the given coordinates. Hence, at each time-interval the algorithm only searches through triangles that are nearby to the rock's coordinates. Then, the first triangle within the impact-threshold is highlighted, and its normal vector and coefficients of restitution are used for bounce modeling. This improvement significantly reduced the overall time of computations in which the longest

trajectory simulation on the largest mesh file takes less than a minute in average computer configurations.

3.5 RPF3D Stopping Criterion

While determining maximum height after each bounce together with rock velocities and kinetic energy are essential for mitigation design, runout zone estimation is the most critical task in rockfall simulation programs for hazard zone identification and evacuation procedures. As a lumped mass method is used in RPF3D, the only stopping criterion that could be considered was the magnitude of the velocity vector. This value can be determined by the user and it can vary for different areas of an open-pit mine based on risk levels for each area.

3.6 Summary

A detailed overview of different aspects of the RPF3D algorithm was presented in this chapter. The key feature of the program is the capability to handle extremely large mesh files that guarantee accuracy of surface geometry for trajectory simulation. Despite the use of advanced algorithms, RPF3D is structured to require minimum possible input data without sacrificing depth of physical modelling provided by other counterpart rockfall programs. RPF3D was developed to be compatible with limited data availability in open-pit mines while still providing an adequate scope of analysis. Along with the standard outcome of any trajectory simulations (*e.g.*, rockfall trajectories, bounce heights and lengths in 2D cross section, and stopping points) a trace map is generated for any desired area in an open-pit mine where the mechanism of rockfalls can be analyzed according to initial location and level of risk associated with that area.

CHAPTER 4 : EXPERIMENTAL ANALYSIS AND RPF3D CALIBRATION/VALIDATION

Due to the complexity of rockfalls with several contributing factors in each bounce, laboratory tests can provide controlled results essential in validating a rockfall program. Hence, as the next stage after developing the RPF3D algorithm, its efficiency is evaluated by means of small-scale experiments designed to provide a preliminary overview of RPF3D in action. This chapter discusses steps taken to build the experimental setup, conduct rockfall demonstration tests, collect data, and perform trajectory simulation. A comparative study for model calibration will also be discussed.

4.1 Experimental Setup

Small-scale rockfall analysis has not been widely practiced as creating smaller scale models of all associated field parameters is impossible; however, such experiments are suitable for investigating a single physical phenomenon in rockfalls. In this research, due to the lack of field data, a small setup was built to focus on rock-surface interaction, bounce heights, and the effect of angular velocity on rock motion. It was important to build a surface with an adjustable slope angle to allow for different testing scenarios. Figure 4-1 shows an overview of the setup which is a platform that can be fixed at a desired slope angle with different surface materials assembled on top of it.

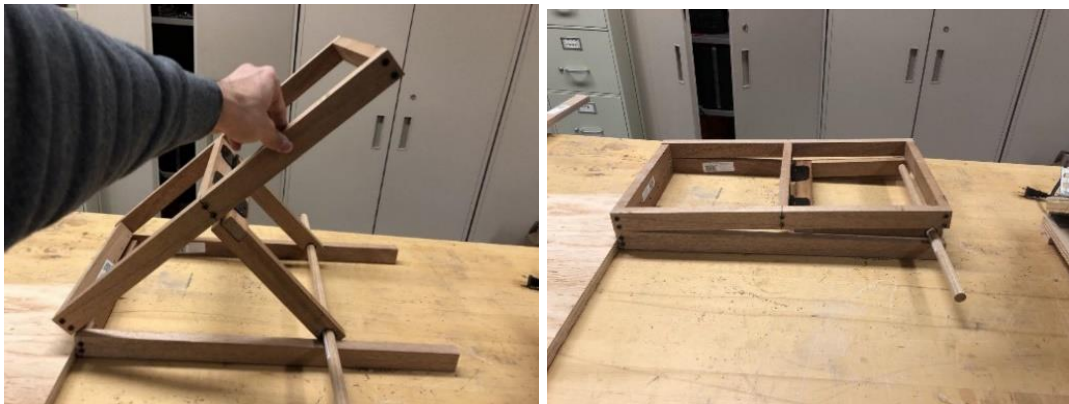
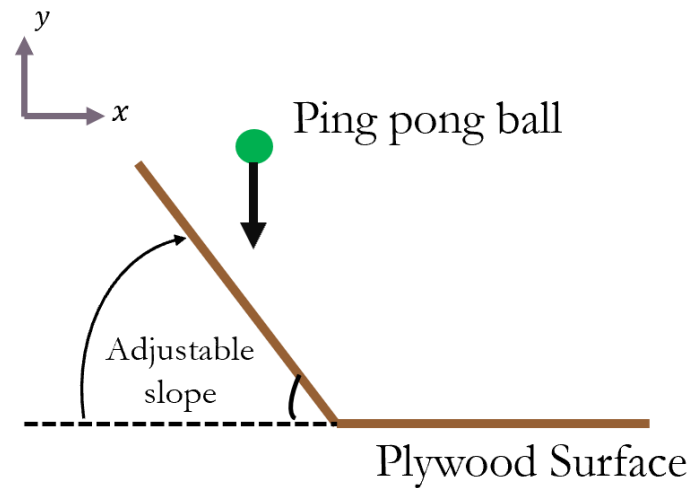


Figure 4-1 Adjustable slope setup for rockfall testing.

As illustrated in Figure 4-1, Plywood was used as the surface of the slope and spherical ping-pong balls were selected for trajectory tests. The plywood can be covered with various surface materials (*e.g.*, cement, soil, rock, *etc.*) and changed as testing requires. Ping-pong balls exhibit high angular velocity at each bounce so that translational and rotational motions can be studied in a more detailed manner. Moreover, spherical samples represent one of the worst-case scenarios in rockfall trajectory analysis due to their excessive runout zones and rolling behavior. Hence, such experiments can be acceptable references for calibration of lumped-mass models where the error percentage of assumptions needs to be identified for further use in large-scale projects.

Each bounce experiment started with the ball released from a pre-determined point above the inclined surface. After bouncing on the inclined surface, the ball continued to bounce on a horizontal surface extending beyond the inclined surface. A maximum of three bounces of the ball were recorded by a high-speed camera for further analysis to determine ball location throughout this process.

4.2 Object Tracking

Tracking algorithms have several applications in traffic control, face recognition, *etc.* as part of computer vision that is a science of programming to process and analyze images and videos. Open Source Computer Vision Library (OpenCV) was initially developed in 1999 to provide optimized techniques for different computer vision applications. For the purpose of this thesis, the OpenCV object tracker algorithm was used to track the ball motion throughout the experiment. This algorithm works with several different key indicators for the object to be tracked. The ball color was used as an indicator for the algorithm to detect the ball in the video. The algorithm then takes video frames and converts them to color space to be able to identify the desired color for tracking. Once the algorithm finds an object with a color within the given HSV range it makes a circle around that area (Figure 4-2).

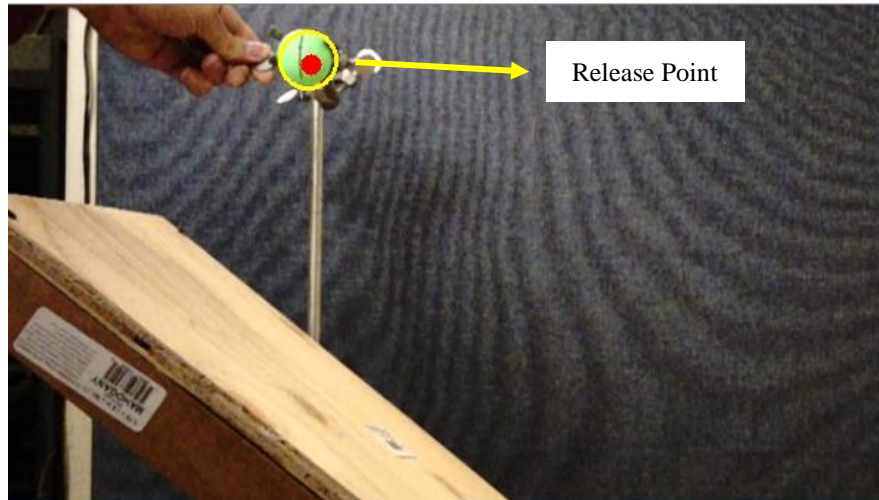


Figure 4-2 Model setup, realising location of the ping-pong ball, and an indication of the object-tracking detection of the ball.

After the ball starts moving, the program follows the circle in each frame and records the circle position in pixels (x,y). After this stage, calibration parameters are used to convert pixel coordinates to real coordinates that identify the position of the ball in reality. Figure 4-3 represents the tracking algorithm while recording ball movements during one of the trials.



Figure 4-3 Object tracking sample using OpenCV. The ball color is used to track the object and the trajectory is superposed.

4.3 Experimental Trials

The objective of the laboratory analysis was to assess/validate the efficiency of RPF3D in finding correct bounce angles, heights and lengths of a moving object given the surface geometry, coefficients of restitution, and initial velocity and location of the ball. Four slope angles were selected in a range of 20 to 60° that are common bench angles of open-pit mines. This range of angles also have the highest impact on COR values (Pavlos Asteriou, 2019). The slope angle was only varied in one direction and the dip direction of the slope remained constant (90°). Several trials were conducted to find the most representative results from the object tracking algorithm and to build confidence in the obtained ball coordinates for each slope angle.

4.4 RPF3D Simulations and Experimental Comparison

A single set of coefficients were utilized for all slope angles to evaluate the program outcome and consistency of results for different surface slopes. Slope geometry was

imported into the program and computation parameters, impact threshold, and time interval were selected according to the scale for each experiment. CORs were derived from simple trial and error tests (on horizontal and vertical planes) to find the best fit of the program outcome to the reality for one of the slope angles (Table 4-1). The 3D trajectories generated by RPF3D simulations are presented in Figure 4-4 for each slope angle.

Table 4-1 Input parameters for lab test simulation.

COR	Initial Velocity Vector (cm)	Impact Threshold	Time-Interval
$R_n = 0.84$ $R_t = 0.70$	(0,0,0)	0.01 cm	0.0001 s

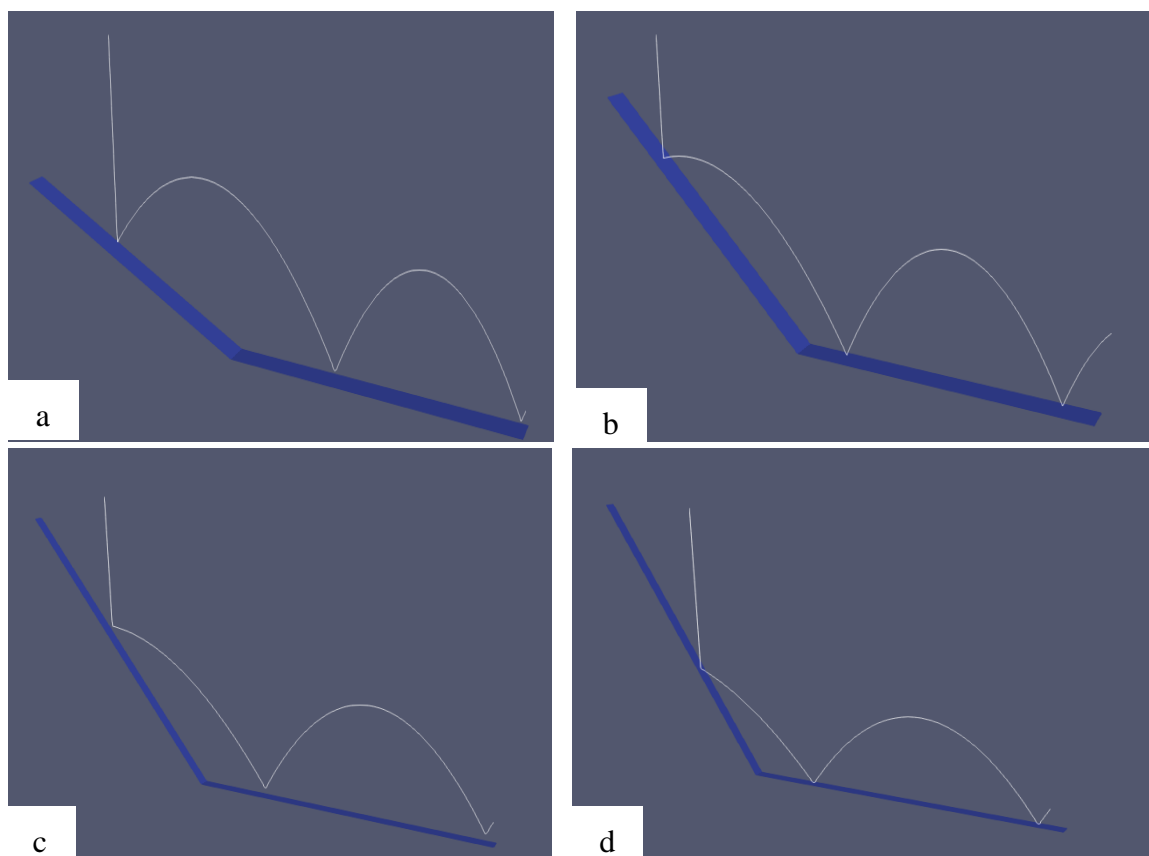


Figure 4-4 The simulations outcome for a)22, b)40, c)50, and d)59° slope angles.

4.5 Comparative Analysis Results and Model Validation

As mentioned in Chapter 3, RPF3D does not consider rotational velocity in rock motion calculation; however, the effect of angular velocity on ball motion was observed in the analysis as slope angles between 20 to 40° have the highest impact on angular velocity of spherical objects (Pavlos Asteriou, 2019). According to lab test results and simulation outcomes, bounce lengths were captured with no more than 8% with the highest error obtained for the 22° slope surface (Figure 4-5). Error was calculated based on the difference between bounce lengths in experimental results and simulation output.

The discrepancy of the results decreases significantly as the slope reaches steeper angles. This can be attributed to the less angular velocity occurring on the ball while impacting steeper slopes ($> 40^\circ$). Figure 4-6 to Figure 4-8 show the other comparative analysis conducted on slope angles of 40, 50, and 59°.

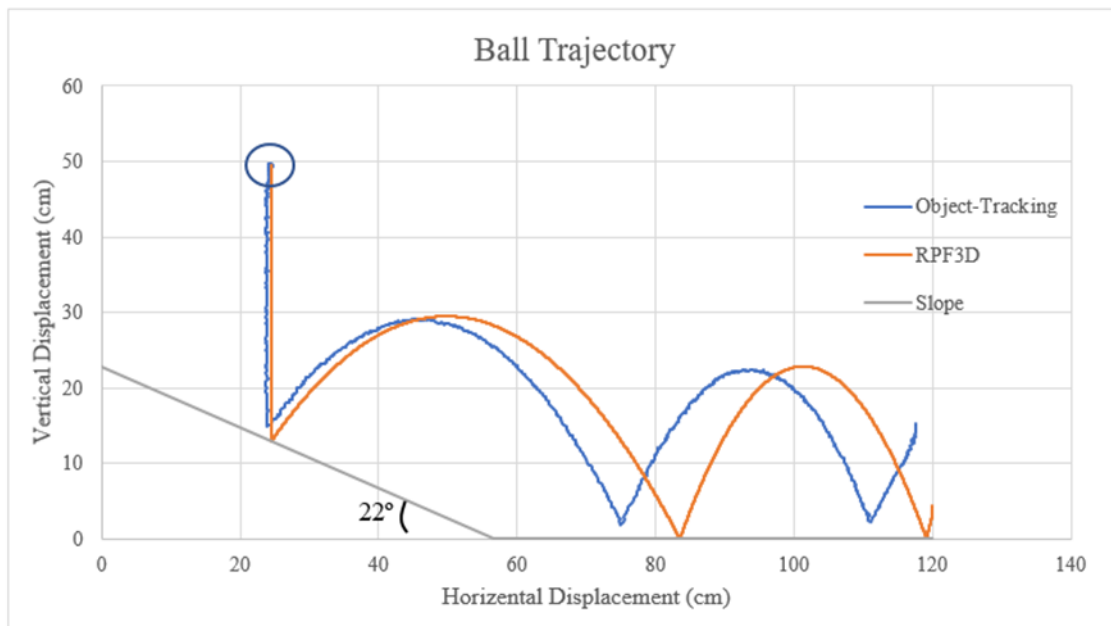


Figure 4-5 Object tracking and computer modeling results for 22° slope angle

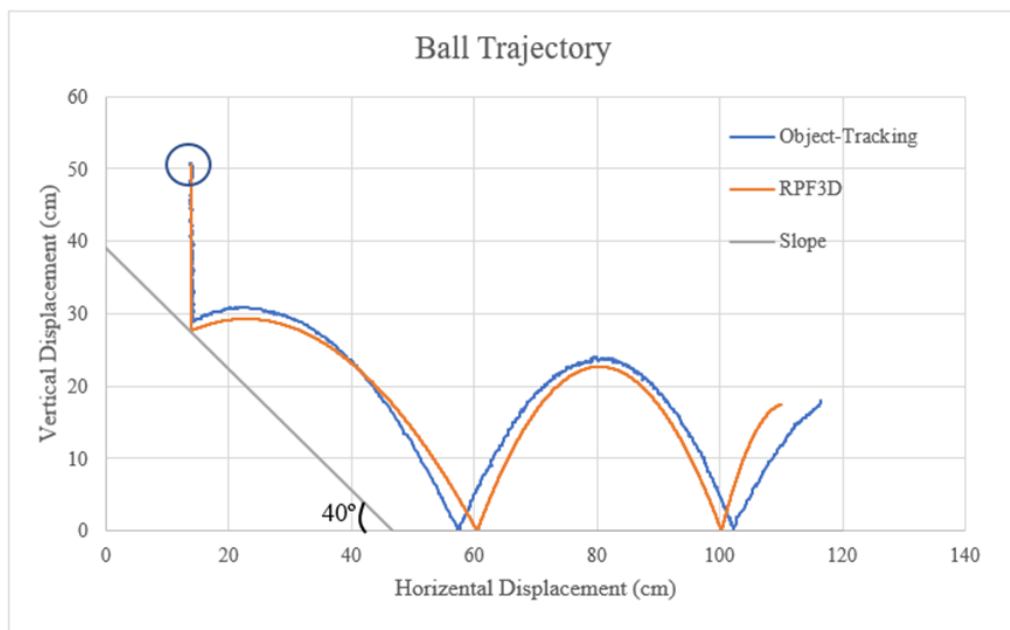


Figure 4-6 Object tracking and computer modeling results for 40° slope angle.

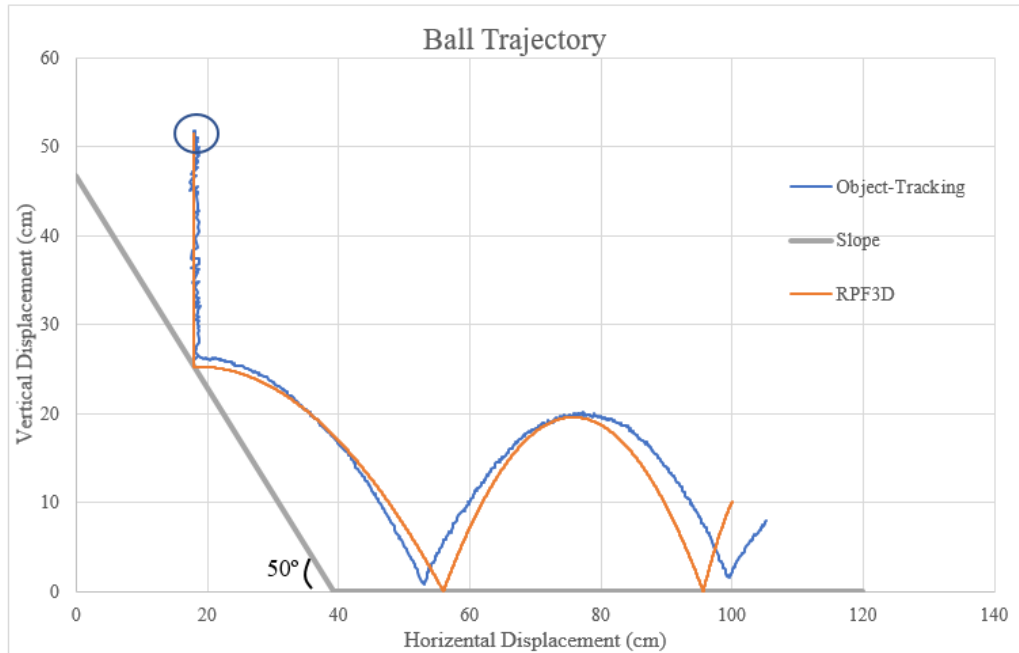


Figure 4-7 Object tracking and computer modeling results for 50° slope angle.

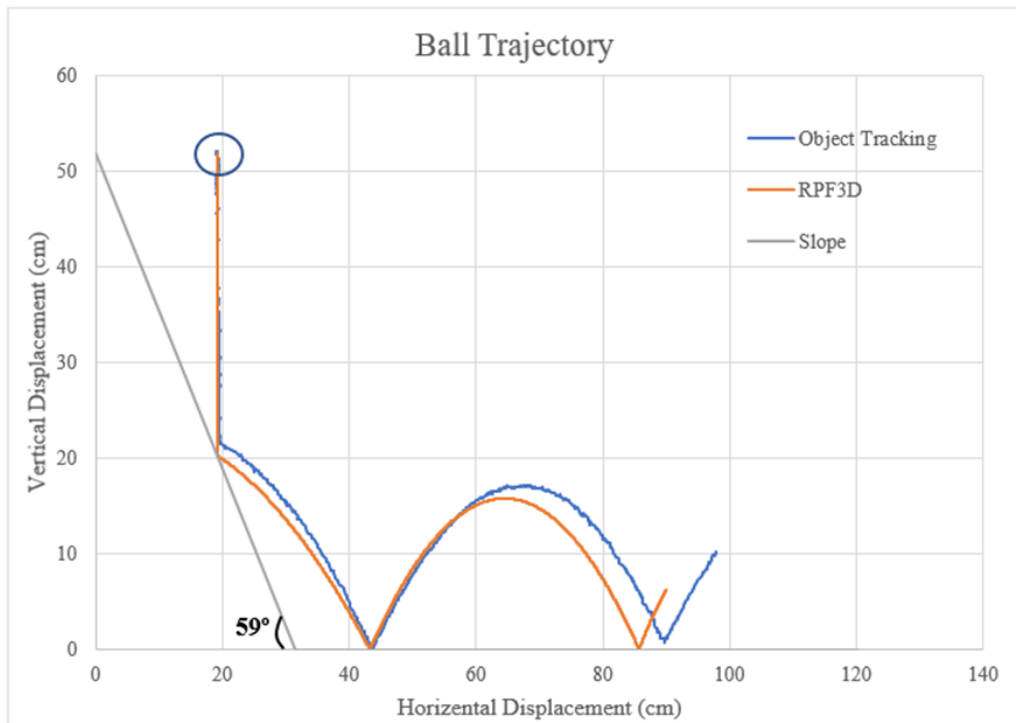


Figure 4-8 Object tracking and computer modeling results for 59° slope angle.

As indicated by these comparison results, observed trajectories spanned a relatively short distance from the releasing point. Therefore, the error percentage is captured in a more conservative manner in comparison to real rockfall incidents where total rock trajectory might extend to several hundreds of meters. For instance, there were a few centimeters of difference in each bounce length between simulation and experimental results that produced 5 to 8% error. Although, the scale effect is still a challenge in validating small-scale experiments, they are nonetheless crucial for calibrating the new computer program.

4.6 Summary

The program outcome was in a good agreement with experimental results. One of the most important parameters in simulating rockfall trajectories is bounce height, which is a vital parameter that must be incorporated in designing reasonable measures for stopping falling rocks before they reach critical locations. Comparative results showed the consistency of RPF3D in simulating bounce heights and rebound directions in small-scale experiments. Errors in bounce lengths on some slope angles were less than 10%, which is not significant. Although the simulated scenarios are far from representing a real scale rockfall incident, they are critical in the first stage of computer program development where essential calibrations are completed.

CHAPTER 5 : APPLICATION OF RPF3D AT AN OPEN-PIT MINE

To evaluate the large-scale performance of the developed program a real open-pit mine was selected and high-resolution aerial images were captured using a quadcopter fitted with an image sensor. This sensor automatically geotags captured images with the WGS 84 (standard U.S. Department of Defense definition of a global reference) coordinate system, helping in the photogrammetric processing of the data. Once the drone lands, the software automatically downloads all images taken during the mission and uploads them to the server where they are processed in Agisoft Metashape software for photogrammetric triangulation. With high-resolution imaging, a 3D pit geometry was produced in STL format (Battulwar et al., 2019).

5.1 Arturo Open-Pit Mine

South Arturo Mine, located in Elko County, Nevada, is owned by Nevada Gold Mines and Premier Gold Mines (companies holding 60% and 40% interests, respectively¹). At this location, large-scale open-pit mining takes place with 110,000 tons of ore and waste moved daily. The primary mineralization is gold ore dispersed in five zones of South Arturo, Dee Deep North, SW Dee, West Button Hill, and Hinge. West Button Hill was explored in 2009 and it was found that mineralization trends north-northeast for over 600

¹ [+https://www.premiergoldmines.com/south-arturo](https://www.premiergoldmines.com/south-arturo)

m in strike length. Figure 5-1 shows the Arturo mine location map and a topographical map for three development phases of this project (Miranda et al., 2018).

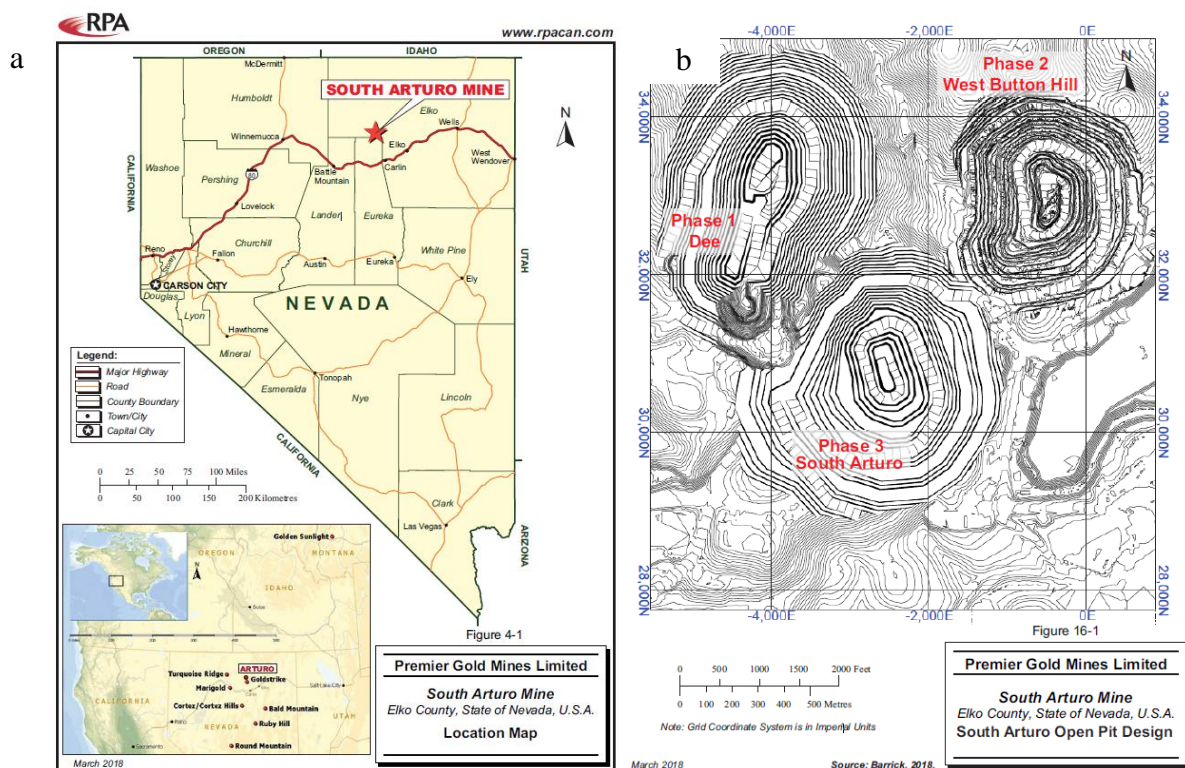


Figure 5-1 a) location map of the Arturo mine, b) open-pit mine design map for three phases of south Arturo mine (Miranda et al., 2018).

Arturo West Button Hill (Phase 2) was selected as the case study for this research. In this phase, the catch (safety) bench width varies from 7.0 m to 9.1 m and bench heights are vary between 12m in waste and 18 m in ore, with a ramp width of 32 m (Miranda et al., 2018). Figure 5-2 shows a high-resolution image of the West Button Hill mine captured for use in photogrammetry.



Figure 5-2 Mosaic aerial photo of the Arturo West Button Hill (phase 2)(Battulwar et al., 2019).

5.2 RFP3D Rockfall Simulation Results

The STL format of the pit topography was used for terrain model construction. Two different resolutions were considered for a comparative analysis to highlight the significance of terrain resolution in trajectory simulation results. The highest terrain resolution included triangles with an average area of 1.0 square meter while lower resolution terrain was composed of triangles with an average area of 20 square meters. Figure 5-3 provides a side-by-side comparison between the two resolutions of the Arturo mine terrain model.

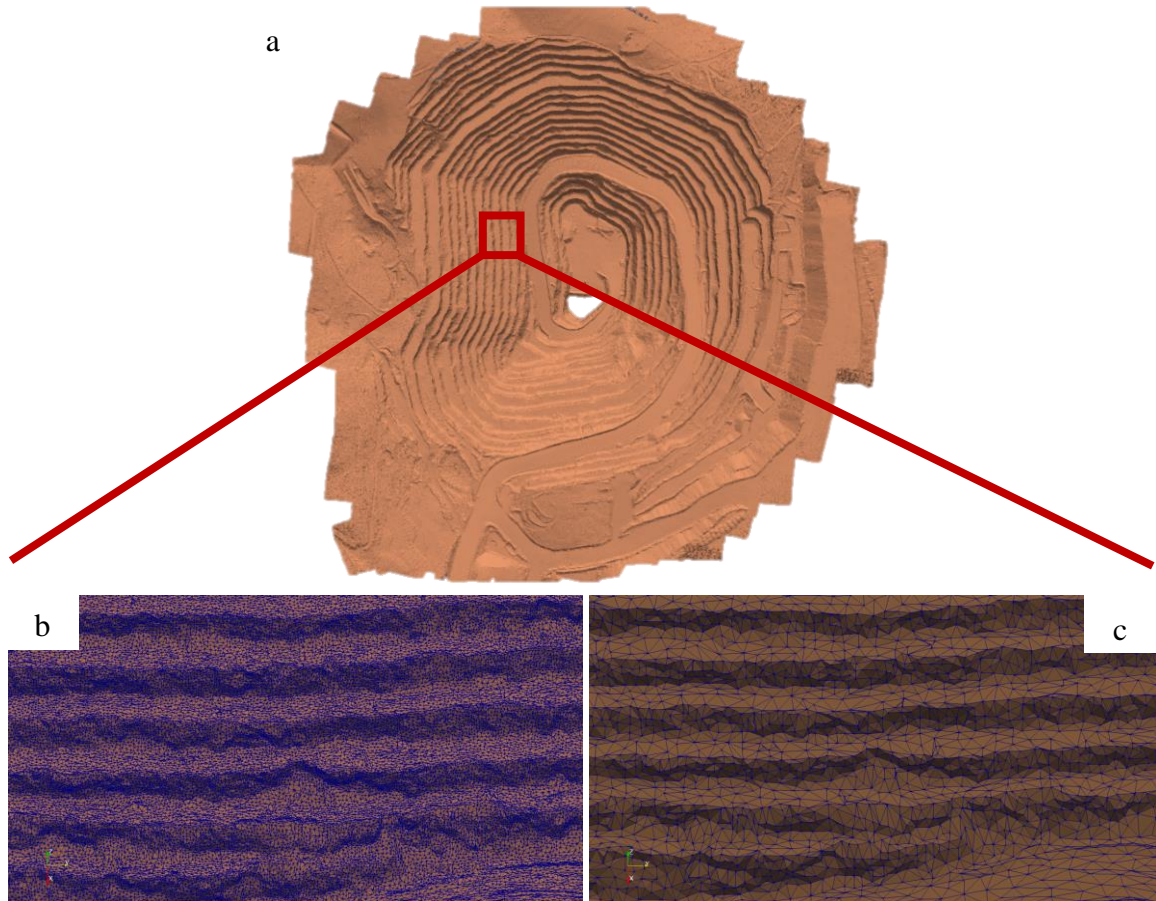


Figure 5-3 a) 3D terrain model, b) Triangles from the high-resolution model (~1 m edge size), and c) Triangles from the low resolution model (~7 m edge size).

Random source locations were selected on the west wall with an altitude of 1687 m. Coefficients of restitution considered for this case were derived from prevalent values in the literature for normal and tangential coefficients. Model parameters were validated using the analytical example provided by Stevens (1998) in developing the rockfall algorithm. Input data and computation specifications are shown in Table 5-1.

Table 5-1 Model inputs and specific parameters for the trajectory computation

COR	Initial Velocity Vector (m)	Source Location Zone	Number of Rock Blocks	Impact Threshold	Time-Interval	Stopping Criteria
$R_n = 0.5$ $R_t = 0.8$	(2,0,0)	West wall, Altitude: 1,687 m	20, Random	0.05 m	0.0001 s	0.5 m

Rockfall trajectories were calculated on both terrain models. Figure 5-4 and Figure 5-5 show the RPF3D output for high- and low-resolution terrain models respectively. It should be noted that model parameters stayed constant for both resolutions and the difference in the outcome is due to the different size of triangles resulting in a change of the terrain model geometry along the rockfall path. Rockfall direction, bounce heights and lengths, and stopping points of each rockfall incident are different for the two terrain models.

In addition to this explanatory case study to show the performance of RPF3D, a comparison was conducted to present differences between high and low resolutions of the terrain model based on three prevalent zones where rock blocks stopped after falling from the 1687 m elevation: first bench, fourth bench, and haulage ramp. Each triangle contacted by the rock is colored white, and highlighted zones are stopping locations. Table 5-2 shows the rock hitting percentage of each designated area for both low and high resolutions.

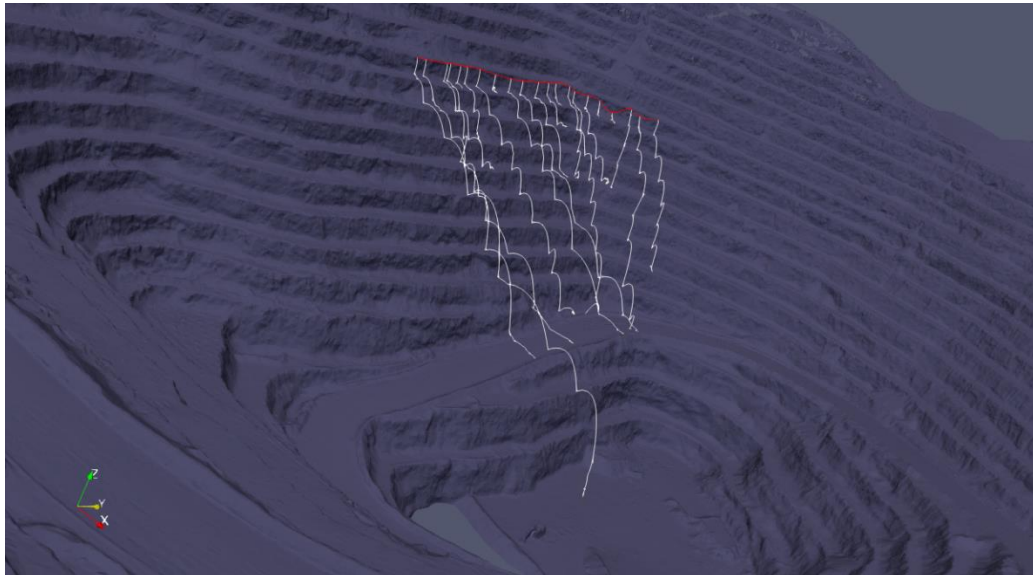


Figure 5-4 Rockfall trajectories for high-resolution terrain.

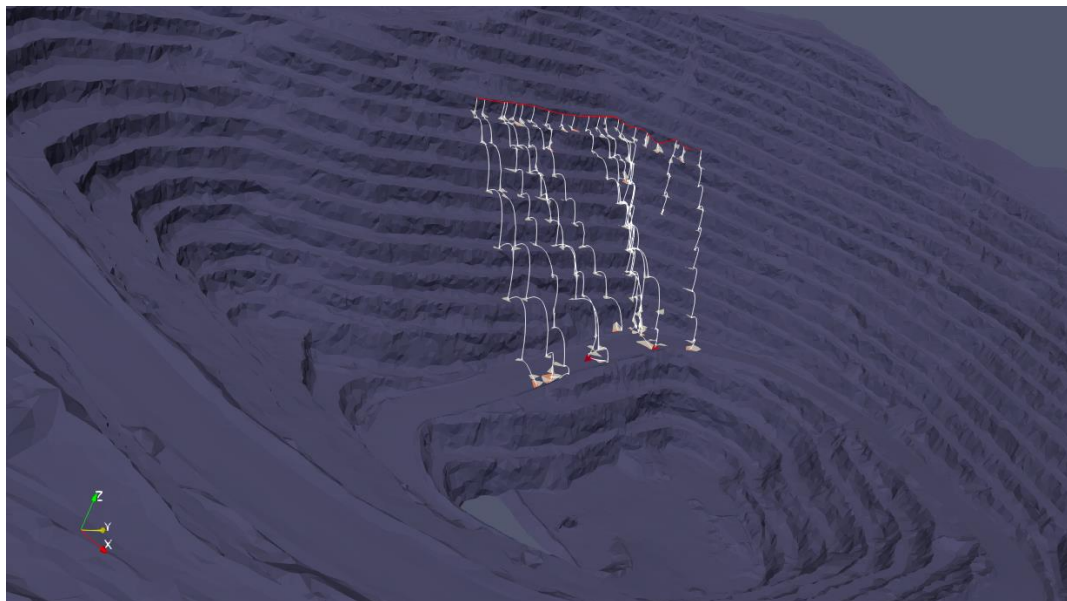


Figure 5-5 Rockfall trajectories for low-resolution terrain.

Table 5-2 Comparative study between two resolutions of the terrain model

Comparative Parameters	Number of Triangles	First bench	Fourth Bench	Haulage Ramp
Low Resolution	150,000	28%	4%	57%
High Resolution	2,332,287	23%	19%	38%

It should be noted that the number of triangles for the lower resolution was selected after testing different resolutions in two other commercial rockfall programs as they exhibited limitation in reading finer mesh files. According to these results, lower resolution exhibited a widely different overview of rockfall runout zones. For instance, 19% of rocks stopped on the fourth bench in the high-resolution terrain model whereas this percentage decreased to 4% in the lower resolution terrain model.

One of the most important objectives of developing such a program is to provide a reliable and easy-to-use rockfall trajectory simulation program. While, performing

complicated dynamic analysis is potentially the primary path for tackling simulation discrepancies with reality, easy and fast simulations on high-resolution terrain models can be more efficient in reaching acceptable results where the intention is identifying hazard zones in a rockfall event. Figure 5-6 and Figure 5-7 provide a closer look at rock traces on the topography. Prevalant locations where rocks stopped are highlighted by yellow ellipsoids to facilitate the interpretation of results.

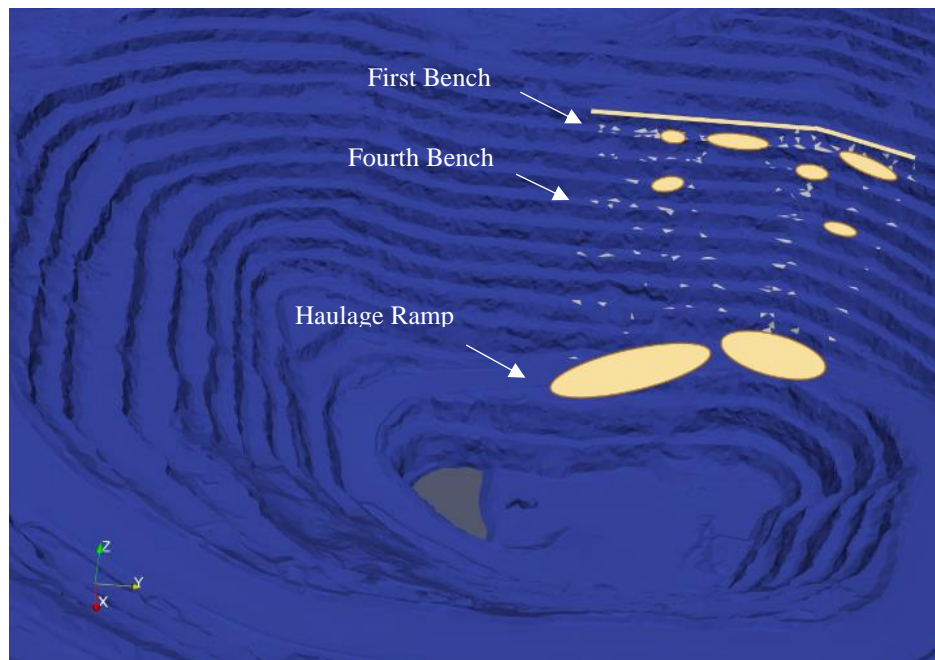


Figure 5-6 Low-resolution pit geometry, rockfall trajectories, and runout zones.

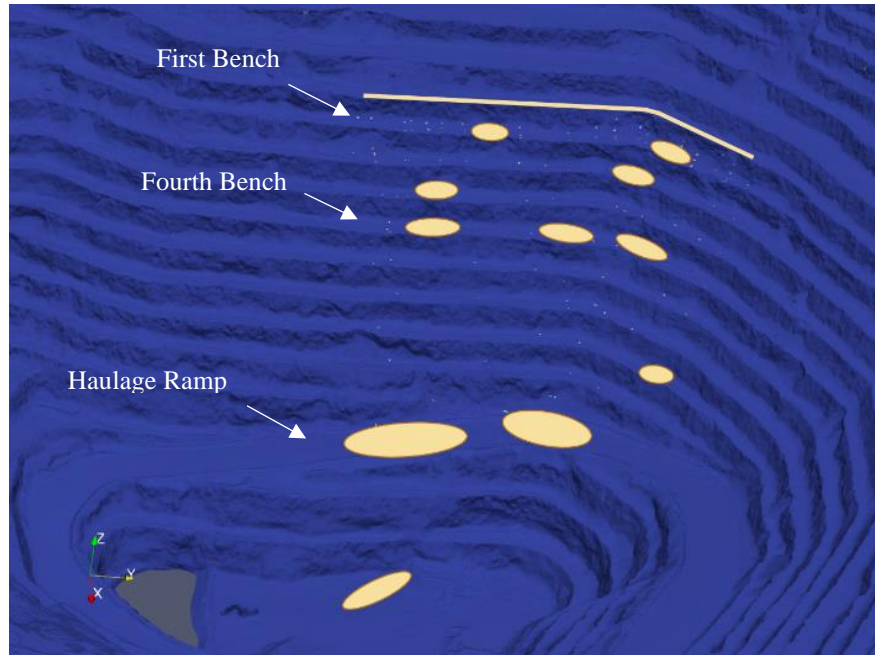


Figure 5-7 High-resolution pit geometry, rockfall trajectories, and runout zones.

As shown in these figures, rockfall trajectories are presented in a trace map format. The difference between resolutions of the two figures can be noticed considering the size of the marked triangles.

Almost a quarter of the rocks stopped on the first bench, which was expected as they are designed to catch rocks after the first couple of impacts; however, 75% of rocks continued on paths to lower benches and 57% and 38% of rocks reached the haulage ramp in low- and high-resolution models, respectively (Figure 5-8). The haulage ramp is the busiest area of an open-pit mine where several vehicles commute during each working shift. It should be noted that in the fine mesh model, one of the rocks went further than the ramp and reached the bottom of the pit, which is alarming for equipment and personnel working in those deeper development areas. More importantly, almost a quarter of the rocks stopped on the fourth bench in the fine mesh model. Knowing this can help when designing preventive berms.



Figure 5-8 Comparison between the outcome for the low and high resolution of the input terrain model.

5.2.1 Effect of local bench spills on the trajectory of the rockfall

The spill formation in open-pit mines is very common on catch benches. They are usually soft materials (soils), altered and weathered rocks, that are detached from the bench face. As these formations are very unstable, it is hard to clean them on the benches and walking or passing by such areas is extremely dangerous. Therefore, as they can mostly result in very small and localized failures, cleaning them is not essential in open-pit mines (Figure 5-9).

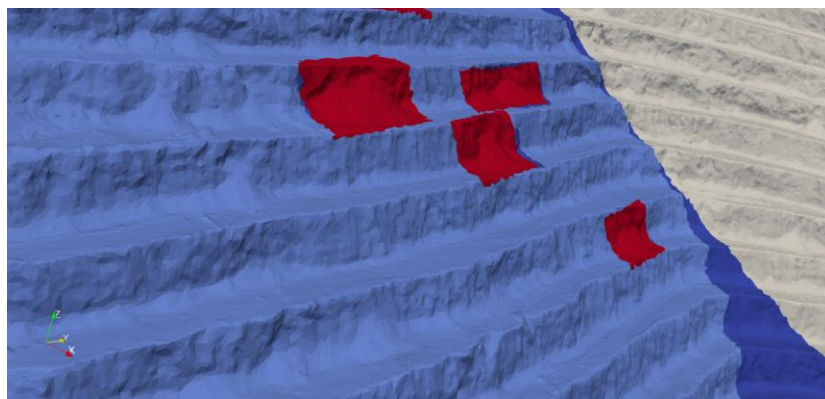


Figure 5-9 A graphical view of the bench scale failures (spills) on the slope walls (red areas).

In rockfall events, however, they can lessen falling speed and intensity by absorbing most of the falling rock's kinetic energy. Hence, the restitution coefficients for these areas are much lower than other parts of the mine. As one of the stages of testing and validating the developed program, special algorithms were designed to allow the user to give different properties to any area of the mine.

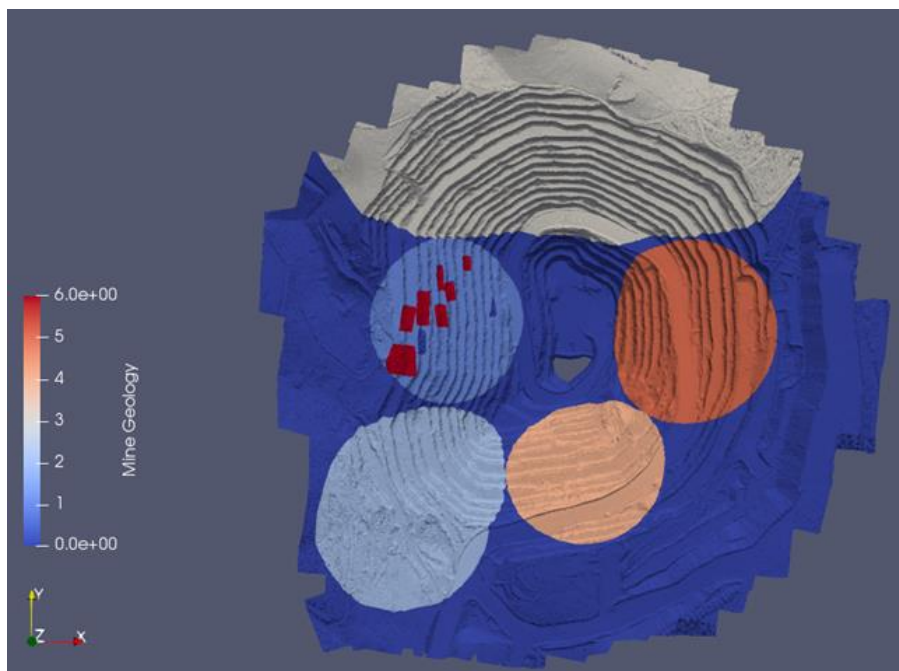


Figure 5-10 Different geological settings and spills detected in red color.

As shown in Figure 5-10, seven arbitrary geology types were assumed for the Arturo mine, where tag number 6 represents spills shown in red color. Coefficients used for each of these geological settings were obtained from conventional properties used in the literature (Wyllie, 2014b). Table 5-3 shows COR values for each geology unit.

Table 5-3 The COR values for each geology unit.

Geology Unit	0	1	2	3	4	5	6
COR	$R_n = 0.5$	$R_n = 0.6$	$R_n = 0.5$	$R_n = 0.4$	$R_n = 0.5$	$R_n = 0.5$	$R_n = 0.25$
	$R_t = 0.8$	$R_t = 0.8$	$R_t = 0.8$	$R_t = 0.7$	$R_t = 0.8$	$R_t = 0.8$	$R_t = 0.4$

The high-resolution terrain model used for the previous case study is selected along with similar model parameters, number of rock blocks and initial locations. This is to emphasize the discrepancy in results for generalized (single) set of COR values used in the initial case study and localized CORs used in the comparative case study. Figure 5-11 and Figure 5-12 show the new computed trajectories on different geological units. As indicated by these figures, rockfall trajectories changed drastically from the initial case.

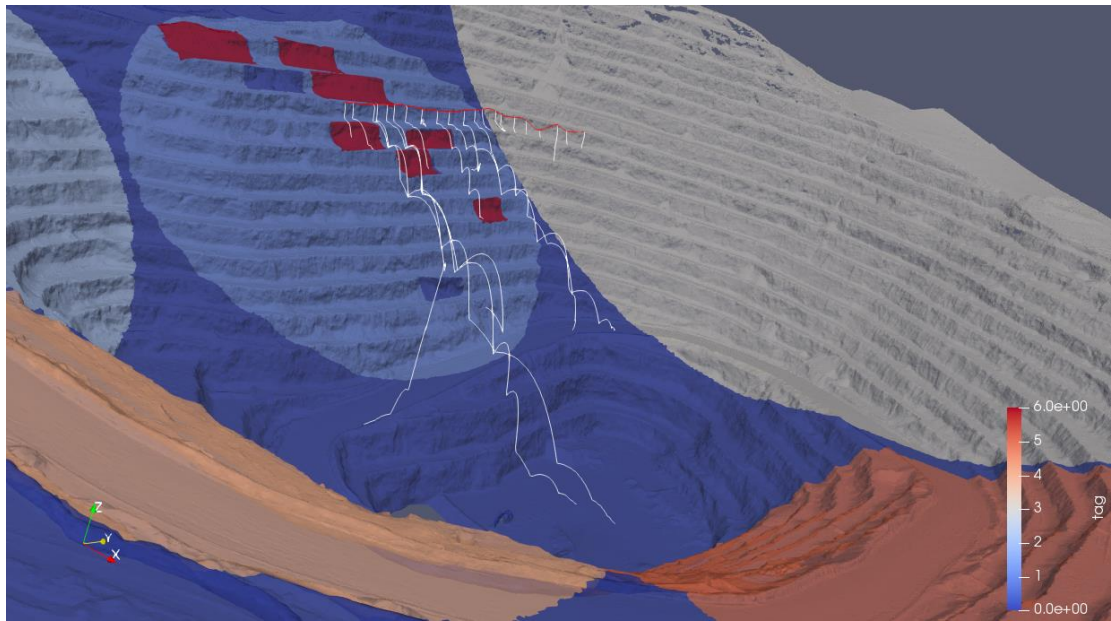


Figure 5-11 Rockfall trajectories on the new terrain model with localized CORs

Figure 5-12 shows the effect of spills on rockfall trajectories. Lower COR values caused rocks to stop higher up on slopes in comparison with the scenario using generalized CORs.

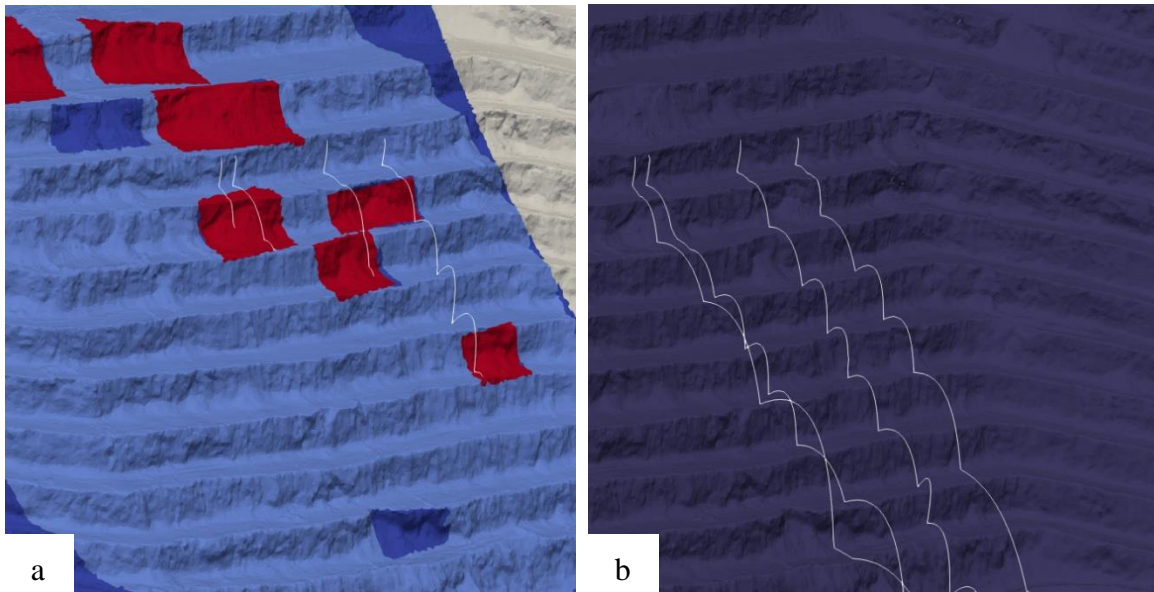


Figure 5-12 Close view of the rockfall trace map a) in a localized COR consideration vs b) generalized COR.

Results show that for the case with localized CORs, 14% of rocks stopped on spills. Selecting a single set of CORs for the terrain model can result in unrealistic results which overlook different types of geologies in an open-pit mine. In the generalized COR model, a higher percentage of rocks reached the haulage ramp. While, 43% of the rocks stopped on first bench in localized COR model, which was an increase of almost double that from the generalized COR scenario. For both cases, less than 10% percent of rocks reached the bottom of the pit. Table 5-4 summarizes simulation results for both models and shows the importance of using accurate COR values. This is further highlighted in Figure 5-13, which shows differences between considering spills and different rock types in the terrain model versus using generalized or localized COR values.

Table 5-4 Results of the comparative study for COR generalizing and localizing.

Comparative Areas	First Bench	Following Five Benches	Following Four Benches	Haulage Ramp	Bottom of the pit
Generalized COR	23%	27%	9%	38%	4%
Localized COR	43%	27%	0%	19%	9%

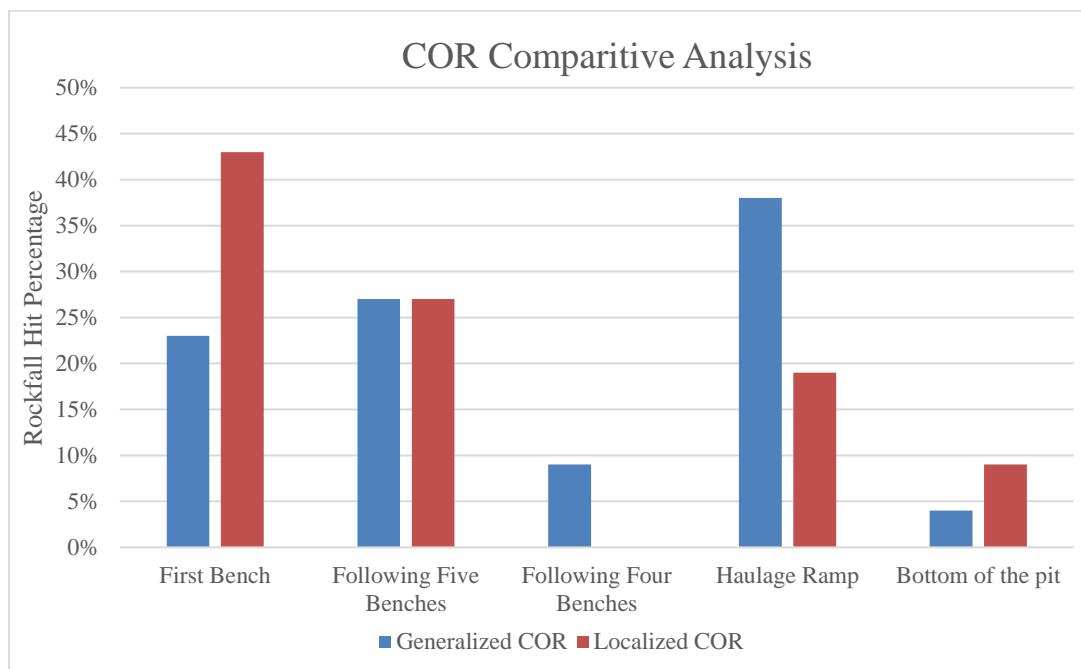


Figure 5-13 Comparison between the two methods of defining coefficients of restitution.

5.3 Summary

The Following points summarize findings in this chapter:

- RPF3D results and performance in working with different terrain resolutions appeared to be as expected. While, similar counterparts of this program are incapable of rendering such heavy terrain models in both STL and DEM format.

- The higher resolution terrain model proved to have tremendous effects on all aspects of rockfall trajectory simulation, which cannot be exceeded by other methods (*e.g.*, stochastic modeling).
- Localized COR values and generalized COR values appeared to play a critical role in trajectory simulation where localized COR values for bench spills were effective in reducing the hitting percentage at the haulage ramp level.

CHAPTER 6 : CONCLUSIONS AND RECOMMENDATIONS

6.1 Research Summary

Details of a new 3D rockfall simulation program, Rock PathFinder (RPF3D), are presented in this thesis. The key feature of the program is the capability to handle extremely large mesh files that guarantee accuracy of surface geometry for trajectory simulation. Despite the use of advanced algorithms in RPF3D, the program is structured to require minimum possible input data without sacrificing depth of physical modeling provided by other counterpart rockfall programs. RPF3D was developed to be compatible with limited data availability in open-pit mines while still providing an adequate scope of analysis. Along with the standard outcome of trajectory simulation (*e.g.*, rockfall trajectories, rockfall velocities, bounce heights and lengths in 2D cross section, and stopping points), a trace map is generated for any desired area in an open-pit mine where the mechanism of rockfalls can be analyzed according to initial location and level of risk associated with that area.

6.2 Research Results

The program's modelling output was in a good agreement with experimental result. Among the most important parameters in simulating rockfall trajectories are rockfall velocities and bounce height, the knowledge of which significantly helps when incorporating reasonable measures for stopping rock before it reaches critical locations. Comparative results from small-scale experiments in bounce height showed the consistency of the RPF3D program. Errors in bounce lengths on some slope angles were

less than 10% which is not significant. Although simulated scenarios were far from representing a real full-scale rockfall incident, they are critical in the first stage of computer program development where essential calibrations are completed.

RPF3D is still undergoing development; however, promising outcomes have been achieved up to this point. These outcomes are summarized as follows:

- RPF3D integrates implementation of the lumped mass method and advanced rock-surface impact detection algorithms for fast and reliable assessment of rockfall runout zones.
- RPF3D's modelling performance when working with different terrain resolutions appears to exceed that of similar rockfall simulation programs, which are incapable of rendering such heavy terrain models in both STL and DEM format.
- Higher resolution terrain models proved to positively impact all aspects of rockfall trajectory simulation generating results that surpass those produced by other methods (*e.g.*, stochastic modelling).
- Localized COR values and generalized COR values appear to play a critical role in trajectory simulation. Localized COR values for bench spills were effective in reducing the percentage of rocks impacting the haulage ramp.

6.3 Recommendations for Additional Research

There are key stages in developing a reliable rockfall simulation program that provides assurance of effectiveness and credibility of outcome to the mining industry. In-depth analysis is required for physical modelling of rockfalls to achieve greater accuracy in

simulating the real processes of bouncing, rolling, and sliding. However, development of complex input parameters is not readily achievable, especially in open-pit mines. Moreover, the computational effort required for advanced analysis is typically beyond what open-pit mining operations can currently afford. Hence, innovative methods and techniques are required to eliminate or reduce the limitation of input data and, at the same time, conduct advanced rockfall simulation in an effective and timely manner. While still in the early stages of implementing such new techniques, RPF3D was successful in solving the high-resolution terrain model limitation for rockfall trajectory simulations.

This thesis presents results from one case study in which RPF3D was utilized in modeling rockfall hazards in an open-pit mine. Based on this experience, it is recommended that additional full-scale rockfall experiments in open-pit mines are necessary for validating results of RPF3D and similar programs prior to their practical utilization.

REFERENCES

- Agliardi, F., & Crosta, G. B. (2003). High resolution three-dimensional numerical modelling of rockfalls. *International Journal of Rock Mechanics and Mining Sciences*, *40*(4), 455–471.
- Asteriou, P., Saroglou, H., & Tsiambaos, G. (2012). Geotechnical and kinematic parameters affecting the coefficients of restitution for rock fall analysis. *International Journal of Rock Mechanics and Mining Sciences*, *54*, 103–113. <https://doi.org/10.1016/j.ijrmms.2012.05.029>
- Asteriou, Pavlos. (2019). Effect of Impact Angle and Rotational Motion of Spherical Blocks on the Coefficients of Restitution for Rockfalls. *Geotechnical and Geological Engineering*, *37*(4), 2523–2533. <https://doi.org/10.1007/s10706-018-00774-0>
- Basson, F. R. P. (2012). Rigid body dynamics for rock fall trajectory simulation. *American Rock Mechanics Association*, *2*, 1438–1444.
- Battulwar, R., Valencia, J., Winkelmaier, G., Parvin, B., & Sattarvand, J. (2019). High-resolution modeling of open-pit slopes using uav and photogrammetry. *Mining Goes Digital - Proceedings of the 39th International Symposium on Application of Computers and Operations Research in the Mineral Industry, APCOM 2019*, 661–670. <https://doi.org/10.1201/9780429320774-78>
- Bourrier, F., Dorren, L., Nicot, F., Berger, F., & Darve, F. (2009). Toward objective rockfall trajectory simulation using a stochastic impact model. *Geomorphology*, *110*(3–4), 68–79. <https://doi.org/10.1016/j.geomorph.2009.03.017>
- Broili, L. (1976). Relations between scree slope morphometry and dynamics of

- accumulation processes. *Meeting on Rockfall Dynamics and Protective Works Effectiveness*, 20–21.
- Caviezel, A., Demmel, S. E., Ringenbach, A., Bühler, Y., Lu, G., Christen, M., ... Bartelt, P. (2019). Reconstruction of four-dimensional rockfall trajectories using remote sensing and rock-based accelerometers and gyroscopes. *Earth Surface Dynamics*, 7(1), 199–210. <https://doi.org/10.5194/esurf-7-199-2019>
- Chen, G., Zheng, L., Zhang, Y., & Wu, J. (2013). Numerical simulation in rockfall analysis: A close comparison of 2-D and 3-D DDA. *Rock Mechanics and Rock Engineering*, 46(3), 527–541. <https://doi.org/10.1007/s00603-012-0360-9>
- Christen, M., Bühler, Y., Bartelt, P., Leine, R., Glover, J., Schweizer, A., ... Feistl, T. (2012). Integral Hazard Management Using a Unified Software Environment Numerical Simulation Tool “RAMMS.” *Congress Interpraevent*, (January), 77–86.
- Crosta, G. B., & Agliardi, F. (2004). Parametric evaluation of 3D dispersion of rockfall trajectories. *Natural Hazards and Earth System Science*, 4(4), 583–598. <https://doi.org/10.5194/nhess-4-583-2004>
- Cruden, D. M., & Varnes, D. J. (1996). *Landslides types and processes: chapter 3. Landslides: Investigation and Mitigation*,.
- Cui, S. hua, Pei, X. jun, & Huang, R. qiu. (2017). Rolling motion behavior of rockfall on gentle slope: an experimental approach. *Journal of Mountain Science*, 14(8), 1550–1562. <https://doi.org/10.1007/s11629-016-4144-7>
- Dorf, D. (2019). *RAMMS :: ROCKFALL - a modern 3-dimensional simulation tool calibrated on real world data*.
- Dorren, L., Domaas, U., Kronholm, K., & Labiouse, V. (2011). *Methods for Predicting*

Rockfall Trajectories and Run-out Zones. (January).

- Dorren, L. K. A. (2003). A review of rockfall mechanics and modelling approaches. *Progress in Physical Geography*, 27(1), 69–87. <https://doi.org/10.1191/0309133303pp359ra>
- Giani, G. P., Giacomini, A., Migliazza, M., & Segalini, A. (2004). Experimental and theoretical studies to improve rock fall analysis and protection work design. *Rock Mechanics and Rock Engineering*, 37(5), 369–389. <https://doi.org/10.1007/s00603-004-0027-2>
- Guzzetti, F, Reichenbach, P., & Wieczorek, G. F. (2003). Rockfall hazard and risk assessment in the Yosemite Valley, California, USA. *Nat. Hazards Earth Syst. Sci.*, 3(6), 491–503. <https://doi.org/10.5194/nhess-3-491-2003>
- Guzzetti, Fausto, Crosta, G., Detti, R., & Agliardi, F. (2002). STONE: A computer program for the three-dimensional simulation of rock-falls. *Computers and Geosciences*, 28(9), 1079–1093. [https://doi.org/10.1016/S0098-3004\(02\)00025-0](https://doi.org/10.1016/S0098-3004(02)00025-0)
- Heidenreich, B. (2004). Small-and half-scale experimental studies of rockfall impacts on sandy slopes. *Ph.D. Thesis*, 3059, 243. Retrieved from http://infoscience.epfl.ch/record/33529/files/EPFL_TH3059.pdf
- Hu, J., Li, S., Shi, S., Li, L., Zhang, Q., Liu, H., & He, P. (2018). Experimental Study on Parameters Affecting the Runout Range of Rockfall. *Advances in Civil Engineering*, 2018, 1–9. <https://doi.org/10.1155/2018/4739092>
- Jones, C. L., Higgins, J. D., & Andrew, R. D. (2000). *Colorado Rockfall Simulation Program Version 4.0. MI 66*. Denver, Colorado.
- Lambert, C., & Coll, C. (2014). Discrete modeling of rock joints with a smooth-joint

- contact model. *Journal of Rock Mechanics and Geotechnical Engineering*, 6(1), 1–12. <https://doi.org/10.1016/j.jrmge.2013.12.003>
- Lan, H., Derek Martin, C., & Lim, C. H. (2007). RockFall analyst: A GIS extension for three-dimensional and spatially distributed rockfall hazard modeling. *Computers and Geosciences*, 33(2), 262–279. <https://doi.org/10.1016/j.cageo.2006.05.013>
- Lan, H., Li, L., & Wu, Y. (2015). Stochasticity of Rockfall Trajectory Revealed by a Field Experiment Repeated on a Single Sample. *Engineering Geology for Society and Territory - Volume 2: Landslide Processes*, 2, 1–2177. <https://doi.org/10.1007/978-3-319-09057-3>
- Lied, K. (1977). Rockfall Problems in Norway. *ISEMS*, 90, 51–53.
- Matasci, B., Stock, G. M., Jaboyedoff, M., Carrea, D., Collins, B. D., Guérin, A., ... Ravel, L. (2018). Assessing rockfall susceptibility in steep and overhanging slopes using three-dimensional analysis of failure mechanisms. *Landslides*, 15(5), 859–878. <https://doi.org/10.1007/s10346-017-0911-y>
- Miranda, H., Geusebroek, P. A., & Scholey, B. J. Y. (2018). *Technical Report on the South Arturo Mine*. Elko County.
- Nugraha, M. G., Kirana, K. H., Srigutomo, W., Saepuzaman, D., Hapsoro, C. A., & Septiyanto, R. F. (2017). The prediction of rockfall run-out using CRSP 3D: A case study at Gunung Batu, Lembang, West Java, Indonesia. *Pertanika Journal of Science and Technology*, 25(S), 47–56.
- Peila, D., Pelizza, S., & Sassudelli, F. (1998). Evaluation of Behaviour of Rockfall Restraining Nets by Full Scale Tests. *Rock Mechanics and Rock Engineering*, 31(1), 1–24. <https://doi.org/10.1007/s006030050006>

- Peng, B. (2000). *Rockfall Trajectory Analysis - Parameter Determination and Application*. (June).
- Pfeiffer, T. J., & Higgins, J. D. (1990). Rockfall hazard analysis using the Colorado Rockfall Simulation Program. *Transportation Research Record*, 1288(4), 117–126.
- Piteau, D., & Clayton, R. (1976). Computer Rockfall Model. *Meeting on Rockfall Dynamics and Protective Works Effectiveness*, No. 90, 123–125. Bergamo, Italy: ISMES Publication.
- Ritchie, A. M. (1963). Evaluation of rockfall and its control. *Highway Research Record*, (17).
- Schweizer, R. I. L. A., Glover, M. C. J., & Gerber, P. B. W. (2013). *Simulation of rockfall trajectories with consideration of rock shape*. <https://doi.org/10.1007/s11044-013-9393-4>
- Scioldo, G. (1991). ISOMAP and ROTOMAP, 3D surface modelling and rockfall analysis. *Geo and Soft*. Torino, Italy.
- Stevens, W. D. (1998a). *RocFall, a tool for probabilistic analysis, design of remedial measures and prediction of rockfalls*. 143. Retrieved from <https://tspace.library.utoronto.ca/handle/1807/16244>
- Stevens, W. D. (1998b). *RocFall, a tool for probabilistic analysis, design of remedial measures and prediction of rockfalls* (University of Toronto). Retrieved from <https://tspace.library.utoronto.ca/handle/1807/16244>
- Szilvási-Nagy, M., & Mátyási, G. (2003). Analysis of STL Files. *Mathematical and Computer Modelling*, 38(7–9), 945–960. [https://doi.org/10.1016/s0895-7177\(03\)90079-3](https://doi.org/10.1016/s0895-7177(03)90079-3)

- Volkwein, A., Schellenberg, K., Labiouse, V., Agliardi, F., Berger, F., Bourrier, F., ... Jaboyedoff, M. (2011). Rockfall characterisation and structural protection - A review. *Natural Hazards and Earth System Science*, 11(9), 2617–2651.
<https://doi.org/10.5194/nhess-11-2617-2011>
- Whalley, W. B. (1984). *Rockfalls*. In: Brunsden, D., Prior, D.B. (Eds.), *Slope Instability*. John Wiley and Sons. New York.
- Wyllie, D. C. (2014a). Calibration of rock fall modeling parameters. *International Journal of Rock Mechanics and Mining Sciences*, 67, 170–180.
<https://doi.org/10.1016/j.ijrmms.2013.10.002>
- Wyllie, D. C. (2014b). Rock fall engineering. In *Rock Fall Engineering*.
<https://doi.org/10.1201/b17470>

APPENDIX

Rock PathFinder3D – Source Code

```
#read, operation, trajectories, heat-map

import vtk

#basic operations, arrays, ect.

import numpy as np

import math

#read the cell ids and tags

from vtk.util import numpy_support as VN

#used for 3D vector operations, read normals from stl file

from vpython import *

# used for plotting

import pandas

import matplotlib.pyplot as plt

#-----#

norms = [] # used in readnormals function
```

```
random = [] # used in randomize_y function

n=0 #counter for number of trajectories

sourceswitcher = 0

slocationx = []

slocationy = []

slocationz = []

# Input geometry - VTP format (before this, bring the STL in Paraview and just export
it as VTP file format)

vtp_file_path = 'Input_Files\\File-Name.vtp'

stl_file_path = 'Input_Files\\File-Name.stl'

points_file_path = 'Input_Files\\Source-Locations.txt'

# Read the normal vecotrs and store them in an array (norms)

def get_file_length(filename):

    with open(filename,'r') as f:

        for i, l in enumerate(f):

            pass

        return i + 1

def read_normals (fname):

    i=0 #counter

    x=get_file_length(stl_file_path)
```

```

with open(stl_file_path,'r') as f:
    for line in f:
        line=line.split()
        if np.mod (i,7)==1:
            n = line
            if i<(x-1):
                norm=vector(float(n[-3]),float(n[-2]),float(n[-1]))
                norms.append(norm)
            i=i+1

read_normals(stl_file_path)
print(len(norms),' triangles read')

def get_source_location(fname):
    with open(fname,'r') as s:
        for line in s:
            n=line.split()
            sourcelocationx=float(n[-3])
            sourcelocationy=float(n[-2])
            sourcelocationz=float(n[-1])
            slocationx.append(sourcelocationx)
            slocationy.append(sourcelocationy)
            slocationz.append(sourcelocationz)

```

```
#read the vtp file

reader = vtk.vtkXMLPolyDataReader()

reader.SetFileName(vtp_file_path)

reader.Update()

data = reader.GetOutput()

tagID = VN.vtk_to_numpy( data.GetCellData().GetArray('tag'))

n_cells = data.GetNumberOfCells() # number of cells (meshes)

closestPoint = np.zeros((3,1))

cell = vtk.vtkGenericCell()

cellId = vtk.mutable(0)

subId = vtk.mutable(0)

closestPointDist_squared = vtk.mutable(0)

VTKpoints = vtk.vtkPoints()

Locator = vtk.vtkCellLocator()

Locator.SetDataSet(data)

Locator.BuildLocator()

where_particle = vtk.vtkIntArray()

where_particle.SetName('Impacts')

for i in range(n_cells):

    where_particle.InsertValue(i,0)
```

```
def randomize_y (yo):  
    i=0  
  
    for i in range (200):  
        point=yo+2*i  
        random.append(float(point))  
  
def heat_map_generator (n):  
    output_filename='Output_Files\\vtps\\heatmap\\'+str(n)+'.vtp'  
    celldata = data.GetCellData()  
    celldata.AddArray(where_particle)  
    myoutput = vtk.vtkXMLPolyDataWriter()  
    myoutput.SetInputData(data)  
    myoutput.SetFileName(output_filename)  
    myoutput.Write()  
  
def save_plot (x,y,n,title,xlabel,ylabel):  
    df = pandas.DataFrame(list(zip(x,y)), columns = [xlabel, ylabel])  
    df.to_csv ('Output_Files\\CSV_Exports\\'+str(title)+str(n)+'.csv', index = False,  
header=True)  
  
    fig, ax1 = plt.subplots(figsize=[10, 4.8])  
    ax1.plot(df[xlabel],df[ylabel])  
    ax1.set_ylabel(ylabel)  
    ax1.set_xlabel(xlabel)
```

```
ax1.set_title(title)

ax1.grid(True)

plt.savefig('OutPut_Files\\Image_Exports\\'+str(title)+str(n)+'.png', dpi=1000)

plt.close(fig)

#ax1.set_ylim([0, 60])

#ax1.set_xlim([0, 120])

#plt.rcParams["font.serif"] = "Times New Roman"

def bounce(xo,yo,zo,velx,vely,velz,n,threshold,increment,filename,velfile):

    velocity = vector(velx,vely,velz)

    velocityf = vector(0,0,0)

    g=-9.81

    dt=0.1

    x=0

    z=0

    y=0

    stop=0

    #restitution coefficients

    Rn=0

    Rt=0

    trajcount = 0

    # outfile = open('Output_Files\\CSV_Exports\\'+str(filename)+str(n)+'.csv', 'w')
```



```
# outvelfile = open('Output_Files\\CSV_Exports\\'+str(velfile)+str(n)+'.csv', 'w')

posz=[]

posx=[]

posy=[]

veltot=[]

points = vtk.vtkPoints()

while True:

    rate(10000)

    z= zo+velocity.z*dt+(0.5*g*dt*dt)

    x=xo+velocity.x*dt

    y=yo+velocity.y*dt

    velocityf.z=velocity.z+g*dt

    velocityf.x=velocity.x

    velocityf.y=velocity.y

    pt_iso = [x,y,z]

    Locator.FindClosestPoint(pt_iso,      closestPoint,      cellId,      subId,

closestPointDist_squared)

    a= 0.0

    a = a + closestPointDist_squared
```

```
if a < threshold:

    no=norms[cellId] #finds the normal vector of the triangle

    tmp = where_particle.GetValue(cellId) # gets its id

    where_particle.InsertValue(cellId,tmp+1) #mark the triangle

    zonetag=tagID[cellId]

    if zonetag==0.0:

        Rn=0.5

        Rt=0.8

    #else:

        #Rn=0.5

        # Rt=0.8

    if zonetag==1.0:

        Rn=0.6

        Rt=0.8

    if zonetag==6.0:

        Rn=0.25

        Rt=0.4

    if zonetag==3.0:

        Rn=0.4

        Rt=0.7

    #print(zonetag)

    #updating the initial location of the rock
```

```

zo=z

xo=x

yo=y

# axis vectors

v2=vector(1,0,0)

v3=vector(0,1,0)

v1=vector(1,0,0)

# the angle of the normal vector with x and y vectors

pradian= diff_angle(v2,no)

pradiany=diff_angle(no,v3)

# corrected angle

radian = pradian-1.5708

radiany= pradiany-1.5708

#direction correction

if velocityf.z > 0:

    radian=pradian

#update the velocities

normalvelocity=(velocityf.z*cos(radian)*cos(radiany))-
(velocityf.x*sin(radian)) - (velocityf.y*sin(radiany))

tengant1 = (velocityf.z*sin(radian)*cos(radiany)) + (velocityf.x*cos(radian))

tengant2 = (velocityf.z*sin(radiany)*cos(radian)) + (velocityf.y*cos(radiany))

normalafter=normalvelocity*Rn

```

```
tengantafter1=tengant1*Rt
```

```
tengantafter2=tengant2*Rt
```

```
velocity.z=          (tengantafter1*sin(radian))          -
(normalafter*cos(radian)*cos(radiany))+(tengantafter2*sin(radiany))
velocity.x=          (normalafter*sin(radian)*cos(radiany))      +
(tengantafter1*cos(radian))
velocity.y=          (normalafter*sin(radiany)*cos(radian))      +
(tengantafter2*cos(radiany))
```

```
#give highere time interval right after bounce to reduce the toral time
```

```
dt=0.001
```

```
if mag(velocity) < 0.5:
```

```
    #print("ball stops at: ",x,y,z)
```

```
    stop=1 #stoping indicator
```

```
    #output the cells that the ball hit
```

```
    heat_map_generator (n)
```

```
# increas the time interval by time increamentt
```

```
dt+=increament
```

```
#store the rock coordinates in arrays
```

```
posz.append(z)
```

```
posx.append(x)
```

```
posy.append(y)
```

```
veltot.append(mag(velocityf))
```

```
    if stop==1:
        break

for trajcount in range (len(posz)):

    if trajcount%100 ==0:
        points.InsertNextPoint(posx[trajcount], posy[trajcount], posz[trajcount])

save_plot(posx,posz,n,'rock trajectory','x dicplacement (m)', 'z dicplacement (m)')
save_plot(posx,veltot,n, 'rock velocity','x dicplacement (m)', 'velocity magnitude
(m/s)')

output_filename='Output_Files\\vtps\\trajectories\\trajectory #'+str(n)+'vtp'

maxloop = 1000

spline = vtk.vtkParametricSpline()

spline.SetPoints(points)

functionSource = vtk.vtkParametricFunctionSource()

functionSource.SetUResolution(maxloop)

functionSource.SetParametricFunction(spline)

functionSource.Update()

data_a = functionSource.GetOutput()

myoutput = vtk.vtkXMLPolyDataWriter()
```

```
myoutput.SetInputData(data_a)

myoutput.SetFileName(output_filename)

myoutput.Write()

# initial values: xo=-23 , zo=1666 , yo=41 (29 other values), vx=2,vy=0,vz=2,
threshold = 0.05, time increment=0.0001

sourcepoints = vtk.vtkPoints()

def sourcelocations_visualization ():

    maxloop = 1000

    spline2 = vtk.vtkParametricSpline()

    spline2.SetPoints(sourcepoints)

    functionSource2 = vtk.vtkParametricFunctionSource()

    functionSource2.SetUResolution(maxloop)

    functionSource2.SetParametricFunction(spline2)

    functionSource2.Update()

data_a = functionSource2.GetOutput()

myoutput = vtk.vtkXMLPolyDataWriter()

myoutput.SetInputData(data_a)

myoutput.SetFileName('Output_Files\\sourcepoints.vtp')

myoutput.Write()
```

```
def compile_():  
    sourcelocations_visualization()  
    get_source_location(points_file_path)  
    slocationfilelength = get_file_length(points_file_path)  
    for sourceswitcher in range(slocationfilelength):  
        xo = slocationx[sourceswitcher]  
        yo = slocationy[sourceswitcher]  
        zo = slocationz[sourceswitcher]  
        sourcepoints.InsertNextPoint(xo, yo, zo)  
        xvel = 2  
        yvel = 0  
        zvel = 0  
        n = sourceswitcher  
        threshold = 0.05  
        increament = 0.0001  
        filename = 'Trajectories_'  
        velfile = 'Total_Velocities_'  
        print('loading trajectory # '+str(n))  
        bounce(xo,yo,zo,xvel,yvel,zvel,n,threshold,increament,filename,velfile)  
compile_()
```